

University of Texas Rio Grande Valley

ScholarWorks @ UTRGV

Theses and Dissertations - UTB/UTPA

11-2014

Pulsar J0453+1559, the 10th double neutron star system in the universe

Jose Guadalupe Martinez
University of Texas at Brownsville

Follow this and additional works at: https://scholarworks.utrgv.edu/leg_etd



Part of the [Cosmology, Relativity, and Gravity Commons](#), [Physical Processes Commons](#), and the [Stars, Interstellar Medium and the Galaxy Commons](#)

Recommended Citation

Martinez, Jose Guadalupe, "Pulsar J0453+1559, the 10th double neutron star system in the universe" (2014). *Theses and Dissertations - UTB/UTPA*. 52.
https://scholarworks.utrgv.edu/leg_etd/52

This Thesis is brought to you for free and open access by ScholarWorks @ UTRGV. It has been accepted for inclusion in Theses and Dissertations - UTB/UTPA by an authorized administrator of ScholarWorks @ UTRGV. For more information, please contact justin.white@utrgv.edu, william.flores01@utrgv.edu.

Pulsar J0453+1559, the 10th Double Neutron Star System in the Universe

By

Jose Guadalupe Martinez

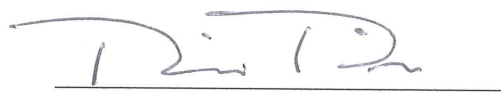
A Thesis Presented to the Graduate Faculty of the College of Science, Mathematics
and Technology in Partial Fullfillment of the Requirements for the Degree of

Masters of Science

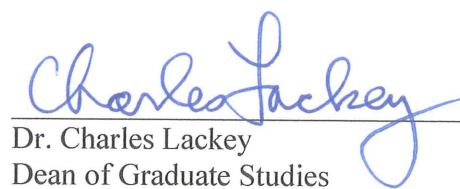
in The Field of Physics

Approved by:



Dr. Fredrick Jenet
Thesis Director

Dr. Richard Price
Name of Committee Member

Dr. Volker Quetschke
Name of Committee Member

Dr. Charles Lackey
Dean of Graduate Studies

Graduate School

University of Texas at Brownsville

Pulsar J0453+1559, the 10th Double Neutron Star System in the Universe

By

Jose Guadalupe Martinez

A Thesis Presented to the

Graduate Faculty of the

College of Science, Mathematics and Technology

in Partial Fulfillment

of the Requirements for the Degree of

Master of Science in the field of

Physics

November 2014

© Copyright

by

Jose Guadalupe Martinez

November 2014

All Rights Reserved.

Glossary of Abbreviations and Symbols

DNS	Double Neutron Star
PSR	Pulsar
TOA's	Time of Arrival's
ARCC	Arecibo Remote Command Center
AO	Arecibo Observatory
Hz	Hertz
K	Kelvin
Jy	Jansky
G	Gauss
M_{\odot}	Solar Mass
P	Period
P_b	Orbital Period
x	Semi-Major Axis
e	Eccentricity
M_T	Total Mass
M_p	Pulsar Mass
M_c	Companion Mass

ABSTRACT

Pulsars are neutron stars that spin rapidly, are highly magnetized, and they emit beams of electromagnetic radiation like a lighthouse out in space. These beams of radiation are only observed when the beams face towards Earth and can be measured by a radio telescope. Pulsar studies have an abundance of scientific implementations in solid state physics, general relativity, galactic astronomy, astronomy, planetary physics and have even opened windows in cosmology.

This thesis reports the results of a study of pulsar (PSR) J0453+1559, a new binary pulsar discovered in the Arecibo All-Sky 327 MegaHertz Drift Pulsar Survey. The recorded observations of the times of arrivals of the pulses of the pulsar in the system, J0453+1559, span a period of about 320 days, which allowed precise measurement of its spin period (45.7 ms) and its derivative ($1.85 \pm 0.13 \times 10^{-19} \text{ ss}^{-1}$). From these measurements we derived the characteristic age of the system as $\sim 3.9 \times 10^6$ years and having a magnetic field of $\sim 2.9 \times 10^9$ G. These measurements point out that this pulsar was mildly recycled by gradual accumulation of matter from the companion star. The cyclic dance of this system has an eccentric ($e = 0.11$) 4.07-day orbit. This eccentricity enables a highly significant quantification of the rate of advance of periastron as $\dot{\omega} = 0.0379 \pm 0.0005^\circ \text{yr}^{-1}$, which entails the total mass of the system as $M = 2.73 \pm 0.006 \text{ M}_\odot$. We also discovered the Shapiro delay, which allows an approximation of the individual masses being $m_p = 1.54 \pm 0.006 \text{ M}_\odot$ and $m_c = 1.19 \pm 0.011 \text{ M}_\odot$, appropriately. These masses, along with the orbital eccentricity, propose that PSR

J0453+1559 is a double neutron star system with a mass asymmetry. The anticipated coalescence time due to the outflow of gravitational waves is $\sim 1.4 \times 10^{12}$, approximately 100 times greater than the age of the Universe. This is the 10th recognized double neutron star system in the known Universe, and below is its story.

Para mi familia,

Thank you for always being there and believing in me, I wouldn't be here today without your advise, support, and your never-ending love. I love you all so much!

ACKNOWLEDGMENTS

I would like to thank Dr. Fredrick Jenet for his invaluable assistance and insights leading to the writing of this work. I thank the Department of Physics & Astronomy at the University of Texas at Brownsville for providing the setting and support that allowed this work to be done. Without the ARCC Scholars program none of this work could have been possible. I am truly grateful for being part of this incredible program and like to truly thank everyone from ARCC Executive Committee, faculty, staff, and students.

TABLE OF CONTENTS

Permission	i
Approval	ii
Copyright	iii
Approval	iv
Abstract	v
Dedication	vi
Acknowledgments	vii
List of Tables	viii
List of Figures	ix
1 Introduction	1
1.1 Pulsar Background	1
1.2 Double Neutron Star Systems	6
1.3 The Lighthouse Model	7
1.4 Pulsar spin evolution	8
1.5 Characteristic Age	10
1.6 Magnetic Field Strength	10
1.7 Pulse Dispersion	11
1.8 Pulsar Population	12
2 Pulsar Timing	14

2.1	Measuring pulse arrival times	15
2.2	Arecibo All-Sky 327 MHz Drift Pulsar Survey	27
2.3	Initial Observations of a New Pulsar	28
2.4	Solving Double Neutron Star System Orbit	33
2.5	Mass Function	35
2.6	Shapiro Delay	40
2.7	Post-Keplerian Parameters and Relativistic Parameters	43
3	Results of J0453+1559	45
3.1	abstract	46
3.2	Introduction	46
3.3	Observations and data reduction	48

LIST OF TABLES

1	Double Neutron Star Systems known in the Universe	8
2	Double Neutron Star Systems known in the Universe	48
3	Timing solutions for PSR J0453+1559.	50

LIST OF FIGURES

1	This is the lighthouse model for a rotating neutron star and its magnetosphere.	13
2	A pulsar's pulses observed at higher frequencies arrive earlier at the telescope than their lower frequency counterparts.	16
3	Diagram showing the basic concept of a pulsar timing observation.	17
4	This figure illustrates the technique of folding. This figure is taken from the Pulsar Search Collaboratory pulsar searching guide.	18
5	Pulsar timing plot examples. In (a) is an example of a good timing solution with no unmodeled effects. In (b) is an example of an error in the frequency derivative. In (c) it shows a sinusoidal ripple that tells us there is an error in position. In (d) it shows that you did not model the pulsar proper motion.	21
6	A prepfold plot of pulsar J0154+18, a millisecond pulsar discovered in the Arecibo All-Sky 327 MHz Drift Pulsar Survey.	25
7	(a) Shows a time series for pulsar J0137+1654 folded at an incorrect period. Notice how the pulse is smeared and has a lower strength detection. (b) The same time series, but folded at the correct period, giving a sharper pulse signal with a stronger detection.	29
8	This is the discovery prepfold plot of pulsar J0453+1559, discovered in the Arecibo All-Sky 327 MHz Drift Pulsar Survey.	31
9	This is the confirmation prepfold plot of pulsar J0453+1559, this strong detection confirmed that PSR J0453+1559 is in fact a real pulsar.	32

10	Barycentric period measurements of PSR J0453+1559 vs time. The black dots denote observations and the red curve shows the expected change in observed period due to eccentric orbital motion for the best fit orbit. . . .	36
11	This plot was created by the online Digital Sky Survey, NASA Infrared Science Archive which shows no optical companion near pulsar J0453+1559 within 5 arcminutes.	39
	41	
13	This plot shows the timing residuals versus its orbital phase of the binary system in which pulsar J0453+1559 is in. The top graph shows the detection of the Shapiro Delay which enables to constrain and measure precise mass measurements of the total mass and companion mass of the system. . . .	42
15	PSR J0453+1559 Timing solution	51

CHAPTER 1

INTRODUCTION

1.1 PULSAR BACKGROUND

Pulsars are rapidly rotating radio objects in the sky that are extremely magnetized, and weigh more than our sun but are only about 10km in diameter, see Figure 1. The formation of neutron stars occurs when stars with a high mass range of 8-20 M_{\odot} go supernovae and leave behind compact and highly magnetized cores. The violent outburst of a supernova blows off the outer layers of a star and creates an alluring supernova remnant. The core of the star then crumples under its own gravity, so protons and electrons fuse under gravity to form neutrons, consequently giving it the name “neutron star”. These particularly condensed objects emit beams of radiation that streak across the sky like light beams from a lighthouse. The term “lighthouse model” is used to describe the underlying idea of the pulsar phenomenon. As the neutron star swiftly rotates, charged particles are accelerated out along the magnetic field lines in the magnetosphere, see Figure 1. This acceleration causes the particles to emit electromagnetic radiation. This radiation is detected on Earth at radio frequencies as a series of observed pulses generated as the magnetic axis of the pulsar, and henceforth the radiation beam, meets the observer’s field of vision with each rotation. The period of the pulses is directly correlated to the rotational period of the neutron star itself.

The discovery of pulsars itself was a major historical event and gave rise to an entirely new field of astronomy. The first pulsar was discovered in 1968 by Jocelyn Bell

and Anthony Hewish [19], since then about 2500 pulsars have been discovered so far. As our technology advances this number keeps increasing.

The first pulsar was discovered by studying the effects of interplanetary scintillation on closed-packed radio sources. Jocelyn Bell's attention was drawn to a pulsed signal with a constant tick of 1.337 seconds. Additional observations found that the signal was consistently detected from the same sky coordinates, its beats were dispersed as anticipated for a signal that journeys through interstellar gas, and the pulses were highly precise, like a heart monitor recording the pulse of a heart that does not skip a beat. After prolonged measurements it was discovered that the pulses did in fact change due to the Earth's orbital motion. At the time, the source of the pulses left people so baffled that they were thought to originally come from aliens, and so it was called Little Green Men 1 (LGM-1). Soon three more heartbeat pulse signals with different spin frequencies and sky locations were uncovered, hinting that more than likely it is a natural occurrence in space rather than Little Green Men. LGM-1 was renamed as PSR B1919+21. The letter B tells you that the coordinates are from the 1950 epoch, which is then followed by the pulsar's sky coordinates. As the search to determine the origin of these pulsars commenced, scientists Thomas Gold and Franco Pacini suggested that these exotic objects were in fact rapidly rotating neutron stars [17] [28]. Soon after radio pulses were detected in the Crab Nebula with a spin frequency of 0.033 seconds. This discovery was the first substantial clue in deciphering how a star becomes a pulsar, hinting at an association between a pulsar and a supernova remnant. The Crab supernova was first observed in 1054 AD, and was reported in cave paintings and portrayed in the pottery of different

cultures around the globe¹ .

Since their discovery, pulsars have been contributing to science, pushing the threshold of the limits of our understanding of our universe. The first extrasolar planets were discovered orbiting pulsars [37]. The stability of the signal received from the pulsar is so consistent, many scientists have decided to use pulsars to investigate one of the most powerful predictions of general relativity: gravitational waves, which are the ripples in the fabric of space-time generated by substantially heavy objects accelerating out in space. The locations of pulsars can be used in interstellar navigation². The engraved plate on the Voyager spacecraft use pulsars to tell of the spacecraft's origin, so should it ever be intercepted by aliens they could find Earth. From planetary to cosmological proportions, pulsars keep uncovering secrets of our universe.

Some of the pioneering discoveries made with pulsars are:

- The first notable discovery with pulsars, is of course the discovery of pulsars itself [19]. Anthony Hewish was later acknowledged with the 1974 Nobel Prize for Physics, for his contribution to Radio Astronomy.
- In 1974, a discovery was made with pulsars that supported the existence of gravitational waves. This discovery was of the first double neutron star system, PSR B1913+16, made by Russell Hulse and Joseph Taylor at the Arecibo radio telescope [21]. This set of neutron stars are dancing around each other in an orbit of 7.75 hours, and in about 200 million years, the pair will merge together due to the outpouring of energy at the price of its orbital decay. The magnitude of the orbital

¹http://www.nasa.gov/multimedia/imagegallery/image_feature_567.html

²http://www.nrl.navy.mil/content_images/06FA5.pdf

decay is about 1 centimeter per day. This was the first test that supported the existence of gravitational waves. Hulse and Taylor were awarded the 1993 Nobel Prize for Physics in recognition of their pioneering discovery.

- The first ultra fast rotating radio pulsar, PSR B1937+21, was discovered by Shrinivas Kulkarni, Donald Backer and collaborators at the Arecibo radio telescope [4]. This neutron star spins at about 642 times per second, this generated a new class of pulsars called millisecond pulsars due to its millisecond spin period. PSR B1937+21 remained the record holder for the fastest spinning neutron star known until 2005. PSR J1748-2446 is currently the new record holder with a spin period of 716 times per second [18].
- The first pulsar discovered in a rich collection of stars known as a globular cluster, was discovered by Andrew Lyne and collaborators at the Jodrell Bank radio telescope [25]. Since this discovery many more pulsars have been found in other globular clusters, which has made it possible to study the physical properties of the clusters using pulsars. An example of a discovery made possible by pulsars is the first detection of ionized gas in the cluster 47 Tucanae [14].
- The first extraterrestrial planetary system was discovered in 1990, which was made possible by PSR B1257+12, by Alexander Wolszczan and Dale Frail at the Arecibo radio telescope [37]. This historic system is comprised of three planets, two Earth-mass planets and one with the mass of our moon.
- PSR B1620-26 allowed for the discovery of the first triple system. The system

includes a pulsar, a white dwarf, and a Jupiter-mass object discovered by Stephen Thorsett and collaborators in the globular cluster M4 [33]. This system gives insight to the rich diversity of evolutionary scenarios feasible in globular clusters.

- In 2003, a double pulsar system was discovered by Marta Burgay and collaborators called PSR J0737-3039 [6]. The binary system is composed of a 22.7 millisecond pulsar in a cyclic orbit of 2.4 hours with a 2.7 second pulsar. This system is a great tool for tests of general relativity.

Many cosmological tests have foretold that the universe contains a low frequency stochastic gravitational wave background created in the big bang era. This stochastic gravitational wave background is the addition of all the gravitational radiation in the universe. Imagine the solar system barycenter and a distant pulsar as opposing ends of an imaginary arm in space. The signal received by the pulsar is used as a reference clock at one end of the arm sending out systematic signals which are recorded by an observer on the Earth. The effect of a gravitational wave passing through the course of the arm would minutely change the local space-time metric and cause a slight change in the recorded signal of the pulsar, similar to a skipped heartbeat while being measured by a heart monitor. Currently there is a world-wide endeavour to detect gravitational waves that is composed of three major collaborations. The three major collaborations are North American Nanohertz Observatory for Gravitational waves (NANOGrav), European Pulsar Timing Array (EPTA) and Parkes Pulsar Timing Array (PPTA). Together these three collaborations are called the International Pulsar Timing Array (IPTA), a consortium of consortia.

For pulsar astronomy being as young as it is, a young astronomical age of 47, it has been an extremely fruitful field of science. The future of pulsar astronomy looks brighter than any pulsar known. As more pulsar surveys continue to become more sensitive, the actual identity of the galactic neutron star population might soon be uncovered. In the near future, many next generation radio telescopes will be operational. The Square Kilometre Array (SKA), which will be operational by 2025 is an example of such a telescope. These telescopes will enable us to see the universe much more precisely. There are many more potential pioneering discoveries to be made in pulsar astronomy, some of them scientists cannot even begin to imagine. To highlight a few discoveries that are expected to be made: the use of millisecond pulsars in the detection of gravitational waves, the first extragalactic pulsar, the uncovering of new double pulsar systems, and the holy grail discovery of the first pulsar-black hole system.

1.2 DOUBLE NEUTRON STAR SYSTEMS

Double neutron star (DNS) systems are scarce and precious physical laboratories that can be used to test relativistic theories. The very first system was PSR B1913+16, which supplied evidence for an orbital decay due to the outpouring of gravitational waves as anticipated by general relativity [21]& [35]. Since then, there have been eight additional double neutron star systems discoveries (all of which are included in Table 2). These systems are unique because you are able to study tests of general relativity and other theories of gravity in the strong-field regime, thus making it the leading system for such research.

A double neutron star system starts its life as two high-mass stars. The older,

more massive star will experience its death in a supernova explosion and give birth to a neutron star that is still accompanied by its high-mass companion. After some time, the high-mass companion star will start to transfer mass onto the neutron star, due to the strong gravitational field of the neutron star. The neutron star will absorb its companion's mass and start to spin up. While this mass transfer is occurring, it can be detected as a high-mass X-ray binary system. After the companion survives the period of mass transfer, it will also end its life by undergoing a supernova explosion, giving birth to another neutron star. The first neutron star created will be recorded as a mildly recycled pulsar, which was spun up by the violent period of accretion from the companion star. The companion star will be recorded as a normal, slower spin period pulsar. These systems are extremely rare due to the fact that both stars survive these violent stages of their life, but the ones that do survive this storm, lead to the creation of a double neutron star system.

This thesis reports the initial timing solution for the newly discovered PSR J0453+1559, which is in a new a double neutron star system. PSR J0453+1559 has a spin period of 45.7 milliseconds and a dispersion measure of 30.3 parsec per centimeter³ and was discovered in the Arecibo All-Sky 327 MHz Drift Pulsar Survey [12], which began in 2010.

1.3 THE LIGHTHOUSE MODEL

The “lighthouse model”, which is a simplified picture of the electrodynamic processes occurring in the pulsars magnetosphere, depicts the characteristics of the discharge of a radio pulsar: its seemingly never ending beat or pulse periodicity, the changes in

Table 1: Double Neutron Star Systems known in the Universe

Pulsar	Period (ms)	P_b (days)	x (lt-sec)	e	M_T (M_\odot)	M_p (M_\odot)	M_c (M_\odot)	Reference
J0737-3039A	22.699	0.1022	1.415	0.0877	2.587	1.338		[6]
J0737-3039B	2773.461		1.516				1.249	
B1534+12	37.904	0.420	3.729	0.2736	2.678	1.333	1.345	[36]
J1756-2251	28.461	0.3196	2.756	0.1805	2.57	1.312	1.258	[13]
J1906+0746	144.071	0.1659	1.419	0.0853	2.6133	1.323	1.290	[24]
B1913+16	59.031	0.3229	2.341	0.617	2.828	1.439	1.388	[21]
B2127+11C	30.529	0.3353	2.518	0.6814	2.712	1.358	1.354	[2]
J1829+2456	41.009	1.76	7.236	0.1391	2.5	1.38	1.22	[7]
J1518+4904	40.935	8.634	0.2495	2.7183	2.62			[29]
J1811-1736	104.1	18.779	34.782	0.828	2.57			[26]
J0453+1559	45.782	4.072	14.467	0.1125	2.73	1.54	1.19	

pulse period, and the narrow beacon of light, see Figure 1. The lighthouse model portrays a greatly magnetized neutron star that is swiftly rotating. The pulsar has a magnetic dipole axis that is inclined with respect to its rotational axis, and the model presents the pulsar’s broadband radio discharge created above the magnetic polar caps in a co-rotating magnetosphere of plasma and is beamed along the magnetic field lines. The recorded “pulse” of a pulsar by a radio telescope is a consequence of one or sometimes both of the beacons of light sweeping past the Earth during its stable rotational cycle, see Figure 1. It should be noted that how pulsars generate their beams of radio and high energy emissions, the formation and configuration of the neutron star itself are still not known definitively [1].

1.4 PULSAR SPIN EVOLUTION

One of the pulsar’s defining properties is the change and evolution of its pulse period, P . This is assuming that consistent loss of rotational kinetic energy occurs. If we consider a pulsar as a straightforward rotating dipole magnet, this “spin-down” is

expected to follow under the rules of classical electrodynamics [22]. A rotating dipole with dipole moment $|\mathbf{m}|$ emitting an electromagnetic wave at the rotational frequency $\Omega = 2\pi/P$. The release of radiation power is given by,

$$\dot{E}_{dipole} = \frac{2}{3c^3} |\mathbf{m}|^2 \Omega^4 \sin^2 \alpha. \quad (1)$$

where α is the angle between the magnetic moment and rotational axis and c is the speed of light.

The rate of rotational kinetic energy loss, known as the “spin-down luminosity”, can be described in terms of the recorded rate of rise of the pulse period, $\dot{P} = dP/dt$, by the subsequent equation,

$$\dot{E}_{rot} = -\frac{d(I\Omega^2/2)}{dt} = -I\Omega\dot{\Omega} = 4\pi^2 \dot{P} P^{-3}. \quad (2)$$

where $I = kMR^2$ is the moment of inertia, the inertia constant, k , the pulsar’s mass, M and the pulsar’s radius R . Usually a value of $I = 10^{38} \text{ kg m}^2$ is assumed. This value correspond to $M = 1.4 M_\odot$, $R = 10 \text{ km}$ and $k = 0.4$, typical values for a pulsar. If it is assumed that all of the rotational energy loss is due to dipole emission, we can identify that equations (1) and (2) give the expected evolution of the rotational frequency,

$$\dot{\Omega} = - \left(\frac{2 |\mathbf{m}|^2 \sin^2 \alpha}{3Ic^3} \right) \Omega^3. \quad (3)$$

Equation (3) is usually written in a more general form in terms of the spin frequency, $\nu = 1/P$,

$$\dot{v} = -Kv^n \text{ or } \dot{P} = -KP^{2-n}. \quad (4)$$

where n is known as the *braking index*, with $n = 3$ for pure magnetic dipole braking and K is a constant.

1.5 CHARACTERISTIC AGE

Integration of equation (4) in terms of the spin period gives,

$$T = \frac{P}{(n-1)\dot{P}} \left(1 - \frac{P}{P_o} \right). \quad (5)$$

where P_o is the spin period of the pulsar at its birth. Under the assumption that $P_o \ll P$ and the pulsar has slowed down solely due to magnetic dipole braking, $n = 3$, the “characteristic age”, which is a rough estimate of the age of the pulsar, can be defined,

$$\tau_c = \frac{P}{2\dot{P}}. \quad (6)$$

For example, the Crab pulsar holds a characteristic age of 1,240 years, which is comparable to its recorded age of about 950 years.

1.6 MAGNETIC FIELD STRENGTH

The conservation of magnetic flux throughout the stellar collapse gives pulsars enormous magnetic field strengths, typically around 10^{12} Gauss. The magnitude of the magnetic field at the surface of the pulsar can be estimated by assuming the spin down is due to dipole braking, and using the relation $B \sim |m| / r^3$. Rearranging equation (3)

gives,

$$B_s = \sqrt{\frac{3}{8} \frac{c^3}{\pi^2} \frac{I}{R^6 \sin^2 \alpha} P \dot{P}}. \quad (7)$$

Assuming $\alpha = 90^\circ$ and using the previously defined values for I and R , gives the expression for the “characteristic magnetic field”:

$$B_s = 3.2 \times 10^{19} G \sqrt{P \dot{P}}. \quad (8)$$

1.7 PULSE DISPERSION

The nature of the journey of a pulsar’s signal through the ionized interstellar medium is dependent upon frequencies that the signal is dispersed out into space. The pulses emitted at lower frequencies arrive later than their higher frequency counterparts. The dispersive delay, t , at radio frequency f (MHz) is given by:

$$t \simeq 4150 \left(\frac{DM}{f^2} \right) \text{ sec}. \quad (9)$$

where DM is the dispersion measure, the integrated column density of free electrons along the line of sight,

$$DM = \int_0^d n_e dl \text{ cm}^{-3} \text{ pc}. \quad (10)$$

where d is the distance to the pulsar and n_e is the number density of free electrons [27].

1.8 PULSAR POPULATION

Pulsars are categorized into two types: slow rotating canonical pulsars and fast rotating millisecond pulsars that coexist in various areas of our galaxy. Eight pulsars exist in the Large and Small Magellanic clouds [8], and eighty pulsars in Galactic globular clusters; the remaining of the known pulsars largely populate the disk of our galaxy. Due to the long wavelength radio waves are easily affected by distances and their propagations through the interstellar medium. Due to this and the fact that the pulsar's radiation beam has to cross the Earth, the current recorded population of pulsars is only a minuscule look at what could be an actual population of 10^6 active pulsars in our galaxy alone. In time, our technology and the spirit of discovery will lead to the discovery of more pulsars in the future.

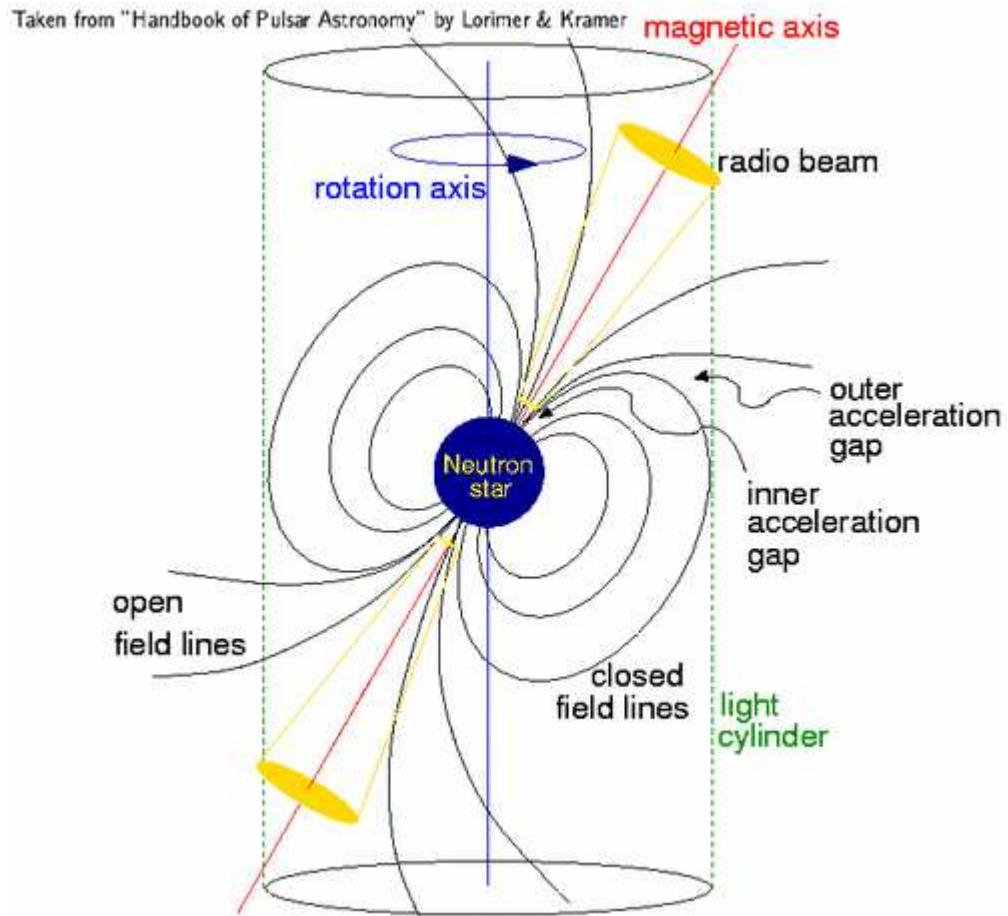


Figure 1: This is the lighthouse model for a rotating neutron star and its magnetosphere.

CHAPTER 2

PULSAR TIMING

Pulsar timing is the regular recording of the rotation of a neutron star by tracking the times of arrival of the radio pulses from the beam emitted by the neutron star as it sweeps over Earth. The high precision tracking of the rotational phase enables pulsar astronomers to study the physics of neutron stars, make exceptionally accurate astrometric measurements, and allows the testing of gravitational theories in unique ways. The Pulsar Timing Array (PTA) is a technique to turn a set of bright, millisecond pulsars into a galactic instrument that is used in the search for gravitational waves. Scientists search for distinct patterns of correlation between the elements of the array. Gravitational waves warp space-time and this distortion effects the time it takes the pulses to travel from the pulsar to a telescope on Earth. We are searching for these disturbances caused by gravitational waves by measuring the variations in the times of arrival of pulses at a telescope, in this sense we are using pulsars as clocks.

We study the arrivals of the pulses from a pulsar that are coming into the radio telescopes and call them times of arrivals (TOAs). From these TOAs it is possible to determine the pulsar's spin period and its derivative. From these two pieces of information, it is possible to derive a pulsar's astrometric parameters. Millisecond pulsars are the most useful of the two types of pulsars in the more extreme applications, because their pulse arrival times can be measured more precisely due to their rotation periods. They are therefore superior clocks for extracting the maximum information from timing

observations.

2.1 MEASURING PULSE ARRIVAL TIMES

The majority of pulsars are weak radio sources, so in order to obtain a significant detection, the incoming pulses collected by the dish of a radio telescope are amplified by highly sensitive receivers, before being de-dispersed and then folded to form a mean pulse profile.

Dispersion is where pulses observed at higher frequencies arrive earlier at the telescope than their lower frequency counterparts, (see Figure 2). Anthony Hewish accurately explained this spreading, or dispersion, of the pulse is due to the frequency dependence of the group velocity of radio waves as they propagate through the ionized component of the interstellar medium. Dispersion was one of the effects first noted in the discovery of pulsars [19].

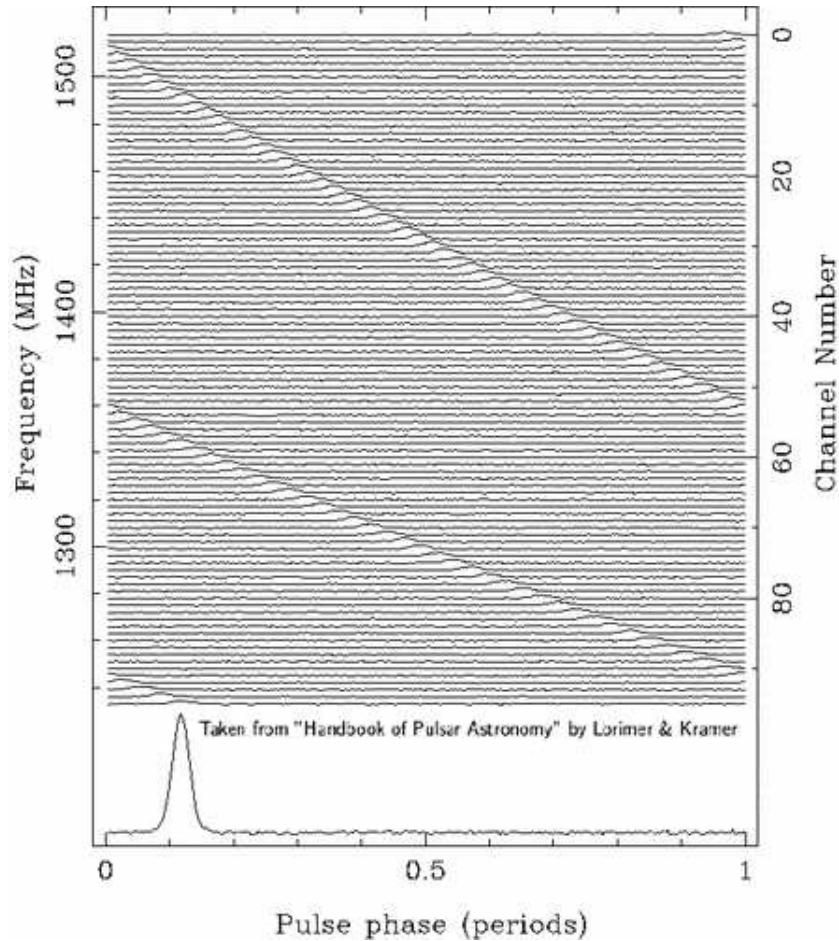


Figure 2: A pulsar’s pulses observed at higher frequencies arrive earlier at the telescope than their lower frequency counterparts.

A fundamental procedure used in pulsar observations is the synchronous averaging, or “folding”, of the data at the pulse period. The additional “folding” of many pulses helps the signal to be amplified above the background noise, an increase that is essential for studying pulses in detail.

From this folding, the time of arrival (TOA) of the pulse at the telescope can be determined. The TOA is defined as the arrival time of the nearest pulse to the mid-point of the observation. As the pulses have a variety of shapes, the TOA must refer to some reference point on the profile, which is taken to be the center of the peak.

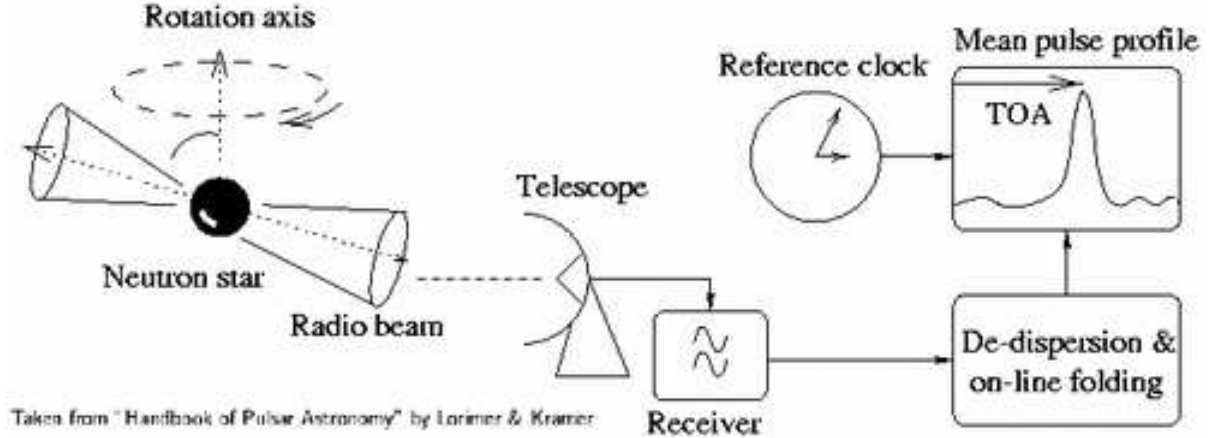


Figure 3: Diagram showing the basic concept of a pulsar timing observation.

In order to explain how “folding” works, let us consider an obsolete method of recording data, which is a long strip of paper that has some data. This paper records marks that tell us the strength of a signal recorded with a radio telescope; the greater the marks on the paper, the stronger the signal. Now let us think of creating these continuous marks while the strip of paper is being pulled along under a pen. The pen will move as signals are detected and it will tell us how strong the signal is. The paper we have described will look something similar to Figure 4.

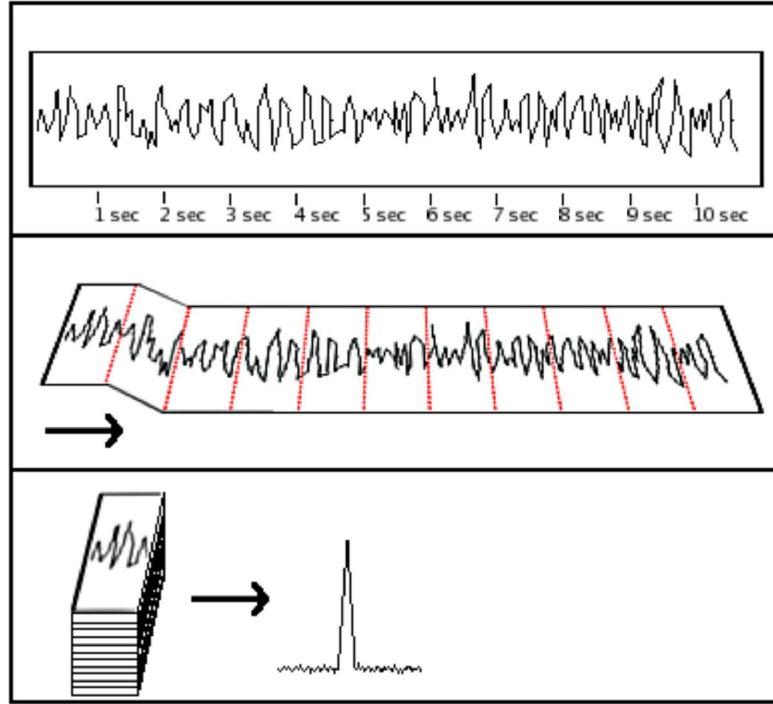


Figure 4: This figure illustrates the technique of folding. This figure is taken from the Pulsar Search Collaboratory pulsar searching guide.

Figure 4 shows marks that are characterized as background noise, but within the background noise is a heartbeat signal from a pulsar is waiting to be discovered. If the pulsar is known and that it has a period of one second, we make marks on the paper for every second following the pulsars heartbeat period. We can now fold the paper on top of itself, so the marks we created line up. Now adding up and averaging the signal in each second, the pulsar's heartbeat signal will be distinguishable from the noisy background that we originally had. However, we usually do not know if there is a pulsar in the data prior to detecting its heartbeats. We then have to do a blind search in every observation and fold it at every possible period and hope to find a pulsar.

This tedious and time consuming work is shorten by using a mathematical tool known as the Fourier transform. The Fourier transform is a set of mathematical oper-

ations that can find periodic signals. It transforms the data from its original form of a signal as a function of time to a form of a signal as a function of frequency. The reason we transform the original data into the frequency domain is because it will tell us how often some signal repeats itself in a given time frame. For example, if some signal is recorded every second, then its frequency is once per second. When the Fourier transform is working on pulsar data, it searches for the heartbeat signals in the frequency domain. If it finds something interesting that could possibly be a pulsar signal, we can look back and fold the data in the time domain to see whether or not it is in fact a pulsar signal. This is a more efficient technique that will save us time in searching for pulsars.

Now that we have reached a better understanding as to how to search for pulsars, let us refer back to the pulsar timing aspect. The main idea to remember about pulsar timing is that it accounts for every single rotation in the neutron star's life and its future rotations. This distinct and precise monitoring of the rotational phase of a pulsar allows us to study them and how they change over time.

One of the first things we measure in pulsar timing is the rotational phase of the pulsar by recording the pulsar's pulse times of arrival, containing an interger number of rotations. Using these TOAs, we now try to mathematically try to figure out the pulsar's rotational phase $\phi(t)$ by approximating it in a Taylor expansion,

$$\phi(t) = \phi_o + f(t - t_o) + \frac{1}{2}\dot{f}(t - t_o)^2 + \dots, \quad (1)$$

where ϕ_o and t_o are arbitrary reference phases and times for each pulsar.

To be accurately measured, $\phi(t)$ must undergo many corrections to the recorded

times of arrivals. We first record the pulses at the radio telescope on Earth in the topocentric inertial frame, a recorded measurement from a fixed position on Earth's surface at time t_t . This time can be corrected by a time t into the inertial solar system center of mass, better known as the barycentric frame, which is typically presumed to be almost the same time as the frame moving with the pulsar. But, we must consider that the recorded pulse heartbeats will be shifted from the actual pulse as it was emitted from the pulsar by an unknown Doppler factor.

$$t = t_t - t_{t_o} + \delta_{clock} - \delta_{DM} + \delta_{R_\odot} + \delta_{E_\odot} + \delta_{S_\odot} + \delta_R + \delta_E + \delta_S. \quad (2)$$

Here t_{t_o} is a reference epoch, δ_{clock} represents the clock correction that considers the differences between radio telescope clocks and terrestrial time standards, the δ_{DM} is the dispersion delay caused by the interstellar medium, the δ_{R_\odot} is the Roemer delay in which the light travel time across the Earth's orbit is taken into account, δ_R is the corresponding delay across the orbit of a pulsar in a binary system, the δ_E , is the Einstein delay that accounts for the time dilation from the moving pulsar, radio telescope, and the gravitational redshift caused by the Sun and by planets or by a binary companion, and the δ_S , is the Shapiro delay, the additional time for the pulses to travel through the curved space time containing the Sun, planets, and/or companions. The result of equation (2) is what is known as the expected time of arrival for any given pulse from a pulsar. Any errors within these parameters, the original recorded parameters like its spin frequency and the spin frequency derivative, or the proper motion, can give you systematic errors in the pulsar timing results. The result that is determined from all

these parameters can be plotted as TOAs versus its “residuals”, which are in the phase differences of the recorded times of arrivals from the predicted model of times of arrivals based on the model parameters you use on that specific pulsar. If the timing model for a given pulsar is a 100 percent accurate the timing residual will be zero.

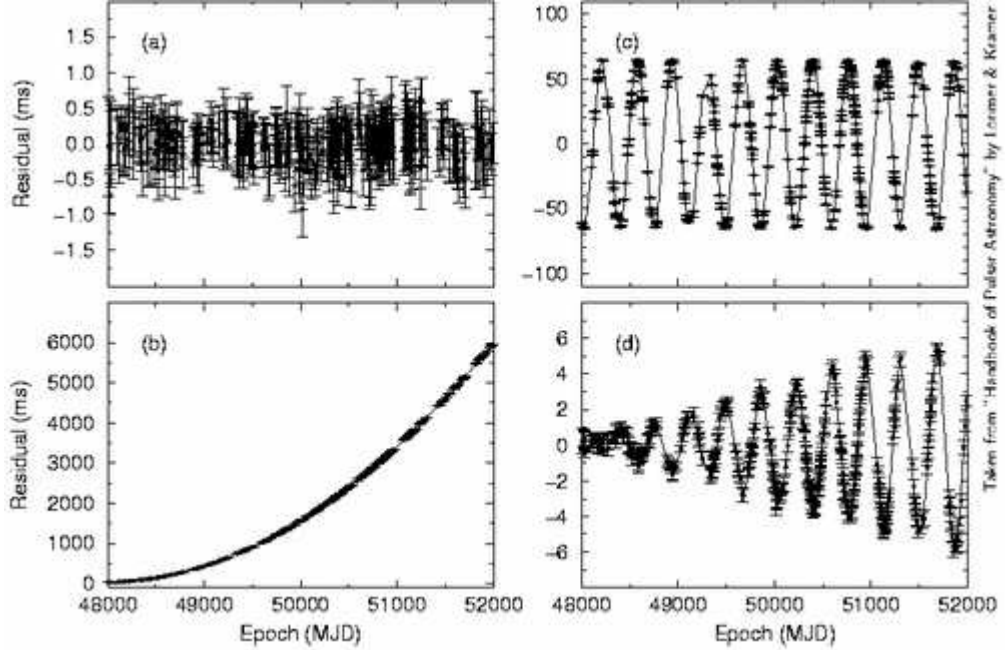


Figure 5: Pulsar timing plot examples. In (a) is an example of a good timing solution with no unmodeled effects. In (b) is an example of an error in the frequency derivative. In (c) it shows a sinusoidal ripple that tells us there is an error in position. In (d) it shows that you did not model the pulsar proper motion.

Pulsar astronomers have collaborated in writing software packages designed for the searching and timing of pulsars using the above techniques. The most popular software package is the Pulsar Exploration and Search Toolkit better known as PRESTO¹. When searching for pulsars PRESTO takes the Fourier transform of a data set and uses software scripts to look for pulsar heartbeat signals within the data. When PRESTO has found a promising candidate, it goes back and folds the data at the hinted period to determine

¹<http://www.cv.nrao.edu/~sransom/presto/>

whether it is a real pulsar or not. The end results could be a collection of beautiful pulsar plots as shown in Figure 6.

PRESTO also includes a number of pulsar tools with which you can create your profile template, make folded plots of your observations done at any major radio telescope, and find the times of arrivals of the pulsar in the data you accumulate. This thesis project heavily used this software package from the discovery of the pulsar until the last recorded times of arrivals of the pulsar. Typically when taking data, the files that are created are Flexible Image Transport System (FITS), which is an open standard defining a digital file format useful for processing of scientific data that is read by **PRESTO**. The FITS files I used contain data taken from Arecibo Observatory, the world's largest radio telescope located in Puerto Rico, when pointing at PSR J0453+1559.

PRESTO has a set collection of scripts designed for the three primary stages of pulsar search analysis. Those used heavily in this project were:

1. Data Preparation

- (a) **rfifind** searches the raw data in both the time and frequency domains for interference or other problems. Each channel is analyzed for short time intervals throughout the observation.

- (b) **prepdata** de-disperses a single time series. This command is useful to prepare the data and is used in **accelsearch** to search for unknown pulsars period.

2. Searching

- (a) **accelsearch** performs a Fourier domain acceleration search with Fourier in-

terpolation and harmonic summing on an FFT. The code is written such that it uses minimal memory. It creates a list of candidates of well detected periodic signals that could be a pulsar.

3. Candidate Optimization

- (a) `prepfold` folds known pulsars or candidates from `accelsearch` over a range of dispersion measures, periods, and period derivative around the best estimated values and returns the optimized pulse profile.

Typically the files generated from the pulsar backend of the Arecibo radio telescope are named in this way: `puppi.MJD_PSRname_OBS_000*.fits`. The `puppi` is the name of the pulsar backend system, `MJD` is the Modified Julian Date, a calendar used by astronomers, `PSRname` is the name of the pulsar that was given, `OBS` is the observation number the pulsar backend system gives, and last is the number of the FITS file.

Among other pulsar timing software packages is one that determines if the beats of a pulsar are comparable to those of its model, and whether the tempo of the times of arrivals of pulsars match the theoretical model. This software program is called coincidentally, `TEMPO` ², and it is used to analyze pulsar timing data. It compares the pulse times of arrival to the TOAs determined by its timing model by using coded input files. After the software is fed with the necessary files it outputs the pulsars parameter values and uncertainties, residual pulse arrival times by using χ^2 statistics and covariance matrix of the model. The χ^2 statistic is a test of how well a fit the

²<http://tempo.sourceforge.net>

model is. The covariance matrix is a measure of how well elements agree with each other from two sets of data move in the similar direction.

When running `TEMPO`, you need two files: an ephemeris file that is the model of the pulsar (ex: `0453+1559.par`) and the actual times of arrivals of the real data of a pulsar (ex: `0453+1559.tim`).

The software analyzes and fits for basic parameters of the pulsar, the first parameters would be its period and period derivative. After having measured a good period and period derivative, all the other pulsars parameters will be derived by those two parameters. If a timing model of a pulsar is already known, using `TEMPO` it is possible to create a more accurate timing model.

The output files one attains after running `TEMPO` are `tempo.lis`, `resid2.tmp`, `matrix.tmp`, and `psrname.par`. The `tempo.lis` is a ASCII format file that lists input parameters, input data (TOAs, frequencies), pre-fit and post-fit residuals, best-fit parameters and uncertainties, statistics, and a covariance matrix. The `resid2.tmp` contains the residuals of the pulsars in binary format for the TOAs, and it includes the TOAs, post-fit residuals, orbital phase, observing frequency, and timing uncertainties. The `matrix.tmp` contains the covariance matrix in binary format of the pulsars parameters. The `psrname.par` is in ASCII format and contains the pulsar's parameters with final values and a fit flag and error for pulsar parameters.

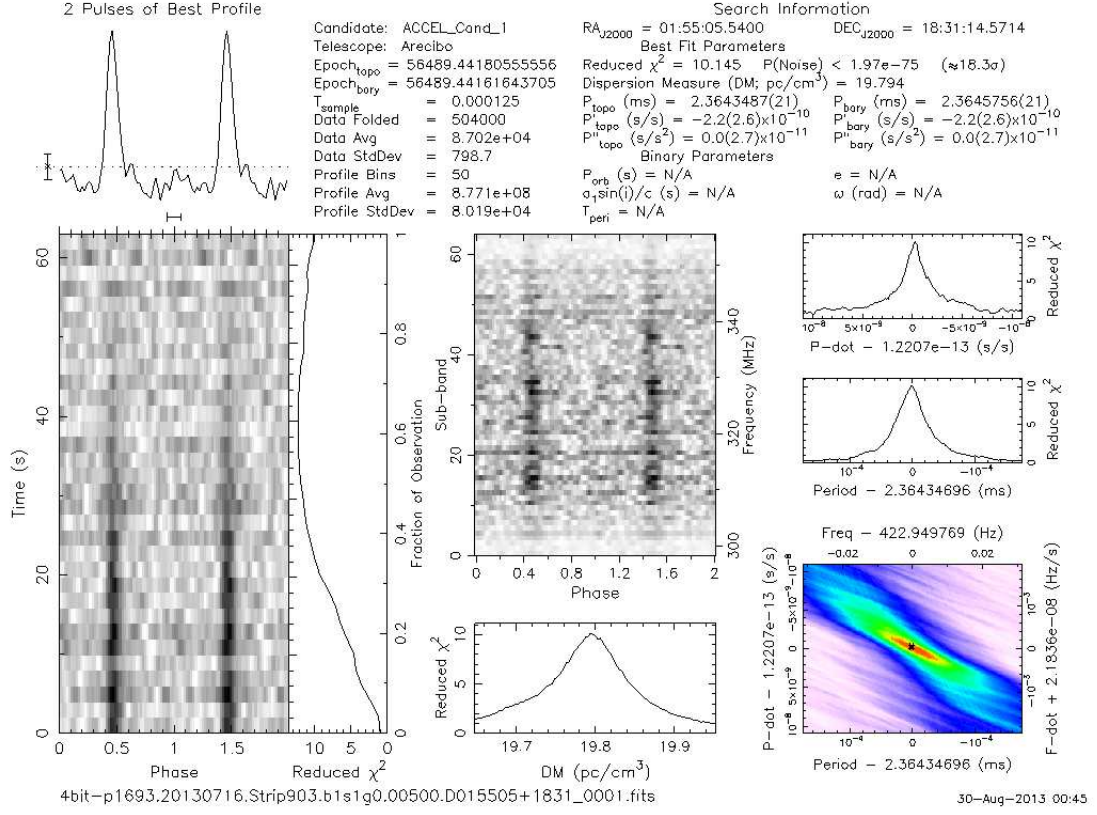


Figure 6: A prepfold plot of pulsar J0154+18, a millisecond pulsar discovered in the Arecibo All-Sky 327 MHz Drift Pulsar Survey.

There are different individual plots in a prepfold plot of a pulsar, see Figure 6. The plot on the upper left is the pulse profile plot, which is the fingerprint of the pulsar after the data has been folded over its period. The plot has two pulse shape heartbeats that have been amplified over the background noise by the folding of the data. The plot located directly below the pulse profile plot is called the time domain plot. It shows the strength of the signal over the course of the observation. Each individual pixel tells us the strength of the signal at that particular time and phase. The signal strength is indicated by the darkness of the bin; the stronger the signal the darker the bin will be.

If the bin is white, it means that there was no signal detected at that time and phase. If there is a pulsar detected in the course of your observation, it will be expected that you would see its strong signal occurring at a consistent phase over the entire observation. In most of the plots that a pulsar was discovered in, the position is slightly off, causing the signal to fade out at the beginning or end of the observation. The time domain plot allows you to decipher the position of the pulsar, due to the fact that the right ascension that the telescope was pointing at is located in the center of this plot. This means if the signal is stronger in the beginning but not at the end of the observation, the right ascension needs to be decreased, and vice versa if the signal is stronger at the end. Directly to the right of the time domain plot is the reduced χ^2 plot that tells you how well a signal was measured in the data.

In the very center of the **prepfold** plot is the frequency versus sub-bands plot. This plot shows the observing frequencies of the receiver that you choose to use for your observations. The plot is composed of the phase of the pulsar versus the frequency, again darker bins mean that a signal was recorded. Typically pulsars are broadband, meaning that they show up in a good range of different radio frequencies. If there is a detection at only a narrow range of frequencies, chances are that it is not a pulsar.

The plot underneath the frequency versus sub-band plot is of the dispersion measure, labeled reduced χ^2 versus DM. The dispersion measure gives us a clue of how far the pulsar signal traveled to get to Earth. Although we are taught to think that space is empty, it is actually filled with a low-density material. This interstellar material is mostly made up of electrons that scatter the pulsar's signal, causing the lower frequen-

cies to arrive later than higher frequencies. The dispersion measure tells us of how much material the pulsar’s signal traveled through, the larger the dispersion measure, the more material it encountered in its journey to Earth and so the pulsar is most likely further away than a pulsar that has a smaller dispersion measure.

These are the major plots used to determine whether a pulsar is real or not. The plots produced by `prepfold` start to tell the story of a pulsar.

2.2 ARECIBO ALL-SKY 327 MHZ DRIFT PULSAR SURVEY

PSR J0453+1559 was discovered using the Arecibo All-Sky 327 MHz Drift Pulsar Survey (AO327). This survey was started in 2010 and utilized the world’s largest radio telescope Arecibo Observatory. A drift survey is one where scientists turn the telescope on and let the Earth’s rotation control the sky that is overhead while taking data. This is often done when the galaxy is overhead due to the fact that it has a multitude of pulsars waiting to be found. An advantage of this type of survey is that can run in the background of other experiments as well, so drift surveys accumulate a lot of data.

The AO327 survey aims to search the entire sky that can be seen by the Arecibo Observatory. This means that the survey is examining the sky between declinations of -1 to 38 degrees, and since its a drift survey, a right ascension field of view of 24 hours. The plan is to do this in two phases. The first phase is to examine the sky between a declination range of 0 to 28 degrees, exluding the region of 10 degrees that the inner Galactic plane exists in. The reason for this exclusion is because Pulsar Arecibo L-band Feed Array Survey (PALFA) already searches this region for pulsars at a frequency of 1.4 GHz. This 1.4 GHz frequency is better suited for pulsar searching in regions where

there is a lot of scattering occurring and hence the pulsars have high dispersion measures. The second phase will extend the survey to the declinations of 28 to 38 degrees, which is the rest of the observable sky by Arecibo Observatory. In order for all degrees of declination to be covered fully, a total of 2707 hours of observation time is required. So far 1413 hours have been completed in this survey. This survey gets approximately 400 hours of telescope time per year, which the set up and slewing of the telescope, as well as the actual data taken, must be completed. This survey is expected to be completed in 2019.

2.3 INITIAL OBSERVATIONS OF A NEW PULSAR

After a pulsar has been discovered, it must be observed additional times to determine its basic properties. The first measurements of a pulsar following its discovery are its period, dispersion measure, and position. The period and dispersion measure are limited to the how well the data was preliminarily folded. Positional uncertainties are usually restricted by the level of the resolution of the radio telescope beam. By reducing the uncertainties in these parameters through additional measurements, the observer is ready for efficient, subsequent observations.

Due to the lack of initial precision in search observations, the pulsar's period may be altered between the discovery and confirmation observations. Reasons for this can be due the discovery of an orbiting companion, or a glitch on the pulsar's spin period. Figure 7 demonstrates what a pulse profile will look like when the spin period of a pulsar is incorrect. It will cause the pulsar's fingerprint profile to broaden and will give the signal a lower strength. Now we consider incrementing the true pulse period by an

infinitesimal time δP so we can determine the rate of change of the period using $\dot{P} = \delta P / P$. This value is small due to the fact that pulsars are extremely stable, but it is possible to detect a rate of change using data that spans a large period of time. This large data set, t_{obs} , allows you to detect slight variations in the times of arrivals, denoted Δt . This can be related to the true period of the pulsar by,

$$P_{\text{true}} = P + \delta P = P + P\dot{P} = P \left(1 + \frac{\Delta t}{t_{\text{obs}}} \right). \quad (3)$$

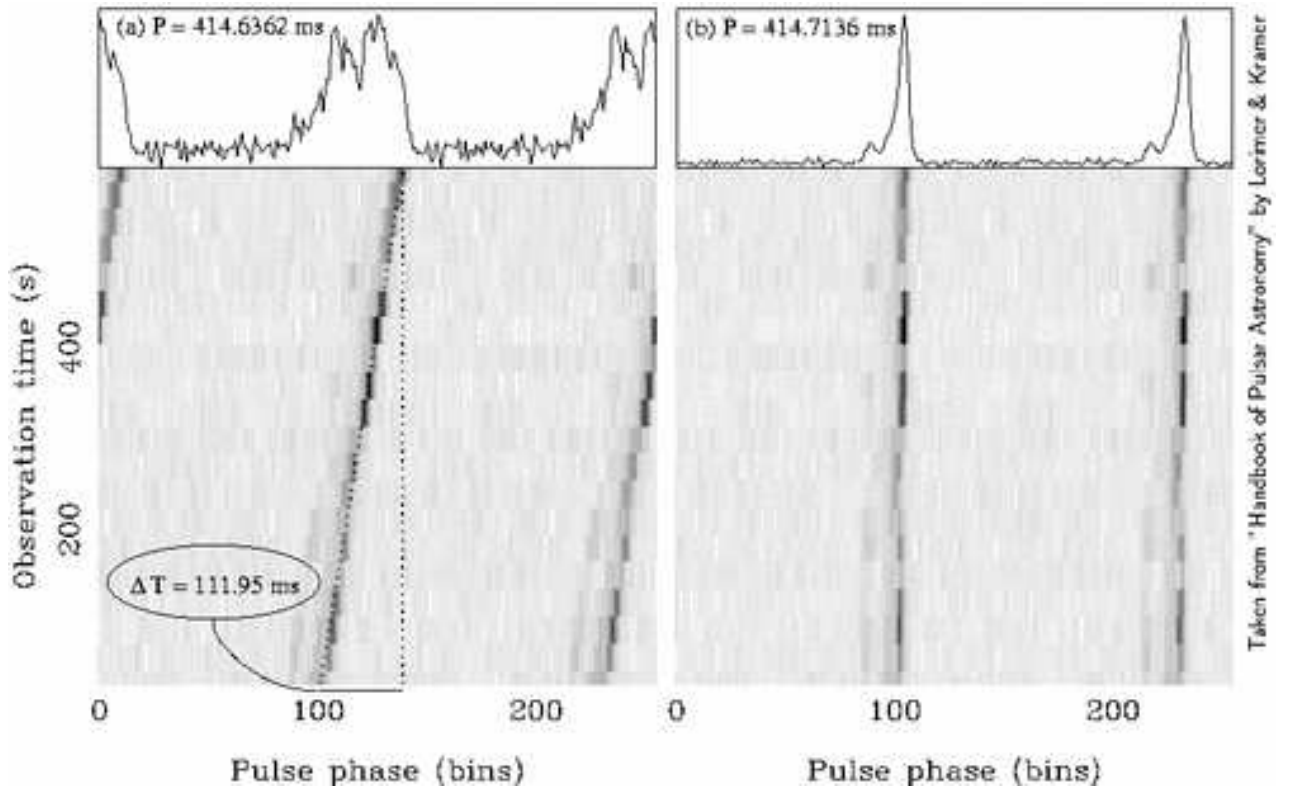


Figure 7: (a) Shows a time series for pulsar J0137+1654 folded at an incorrect period. Notice how the pulse is smeared and has a lower strength detection. (b) The same time series, but folded at the correct period, giving a sharper pulse signal with a stronger detection.

For PSR J0453+1559, its discovery plot showed a weak but resonable signal for a pulsar, see Figure 8. You notice that the pulsar was only displayed in a small fraction

of the time of the observation at that pointing, between 25 seconds - 50 seconds. After having discovered this pulsar, a confirmation observation was needed to determine if it truly is a pulsar. The confirmation observation was done a week after it was discovered. Since in the discovery plot the pulsar only showed up during a small fraction of the observation, it indicated that the initial right ascension of the pulsar was slightly off. This is not expected due to the fact that AO327 is a drift survey. After changing the right ascension slightly and observing the pulsar for a longer time, we get the confirmation plot (Figure 9) showing a true strong pulsar.

Something to note about this pulsar was its unique spin period of 45.7 milliseconds. Many double neutron star systems have pulsars in them with spin periods ranging from 22 milliseconds to 144 milliseconds. This gave good indication towards PSR J0453+1559 being a double neutron star system, but more tests had to be done. Another good indication of it being a double neutron star system is the fact that its spin period changed from 45.77940 milliseconds to 45.769056 milliseconds between its discovery and confirmation. This change in period is a significant one, since isolated pulsars have a very stable periods. When pulsars are in a binary system the period of the pulsar changes due to the Doppler shift as it is orbiting around its companion.

After realizing that this pulsar could be in a double neutron star system, the first thing was to check if there was an optical companion. There are many digital online surveys that have optically mapped out the sky. A popular one is the NASA Finder Chart, which is a visualization tool that allows cross-comparison of images from various surveys of different wavelengths and different epochs. This digital online survey

has access to imaging data sets from the Two Micron All Sky Survey (2MASS), the Digitized Sky Surveys (DSS), and the Sloan Digital Sky Survey (SDSS). We were able to use this in our search for an optical companion. Figure 11 shows that there is no optical component within 5 arcmin of the pulsar, which is a strong indication that this pulsar is not orbiting a white dwarf or a main sequence star, but instead a neutron star.

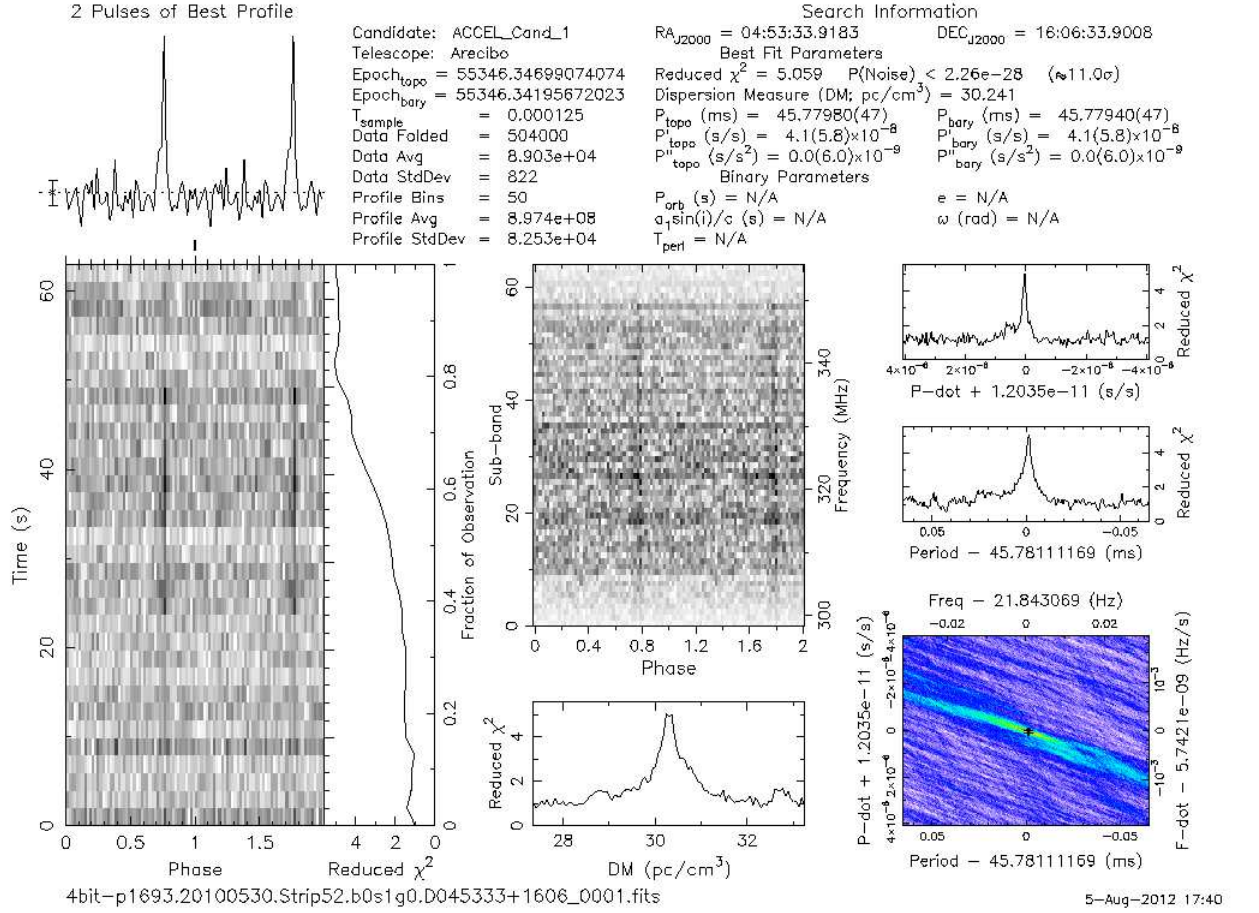


Figure 8: This is the discovery prepfold plot of pulsar J0453+1559, discovered in the Arecibo All-Sky 327 MHz Drift Pulsar Survey.

We now have all of the initial information of PSR J0453+1559, and can now create an ephemeris, better known as a .par file. In this file the pulsar's parameters are placed

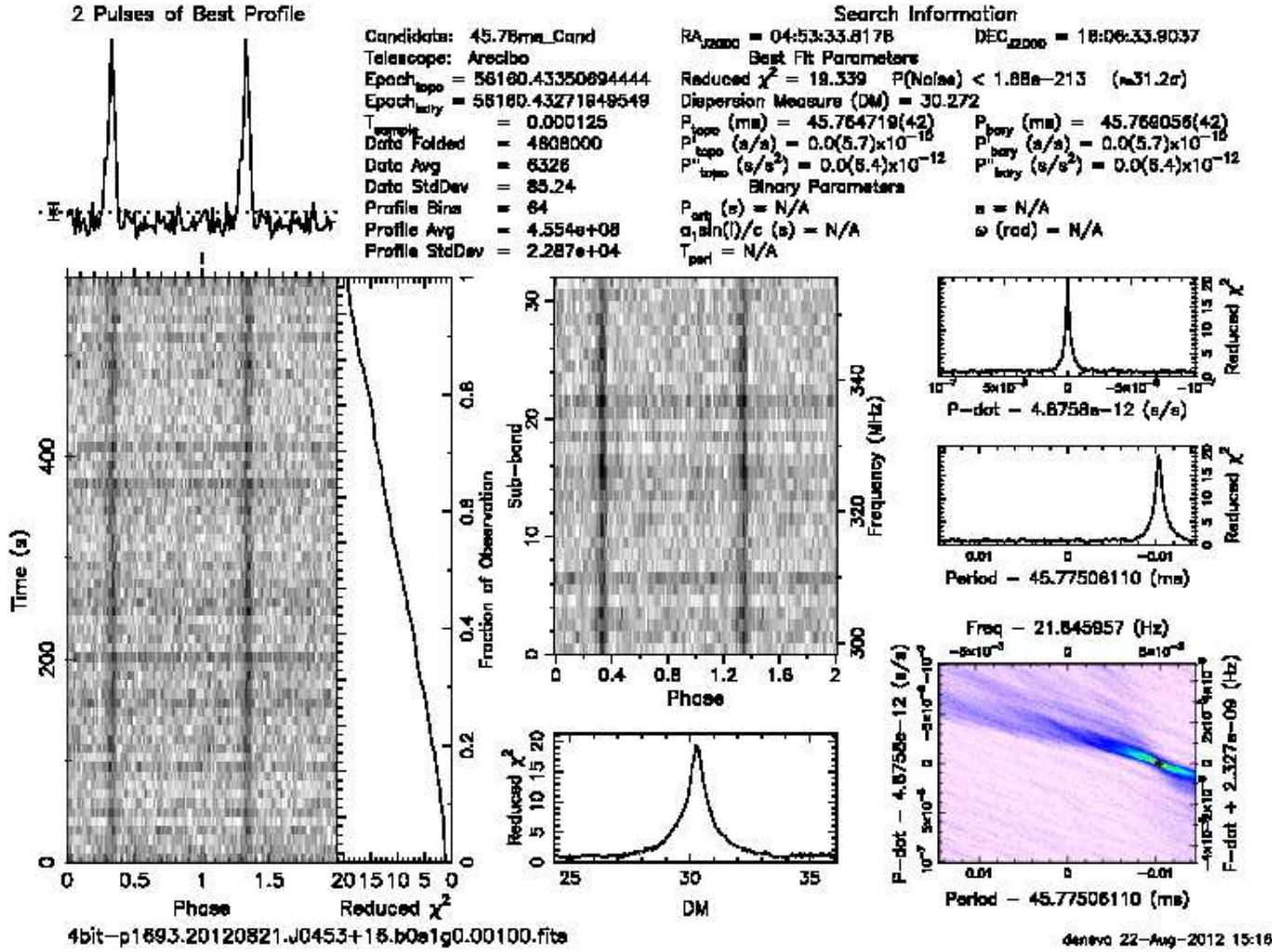


Figure 9: This is the confirmation prepfold plot of pulsar J0453+1559, this strong detection confirmed that PSR J0453+1559 is in fact a real pulsar.

and later are used in solving for more parameters with pulsar software programs like TEMPO. In this initial ephemeris we input its pulsar name, right ascension, declination, spin frequency, and dispersion measure. Later this will include parameters that will be derived from measuring the pulsar's spin frequency and its derivative.

Since PSR J0453+1559 seemed to be a promising candidate to follow up on, a proposal was sent into the Arecibo Observatory to follow up on this pulsar for a whole year. The first months of observing this pulsar were taken in incoherent de-dispersion mode,

due to the uncertainty of the parameters of this pulsar. PSR J0453+1559 was observed with the L-band receiver at the Arecibo radio telescope, which has the frequency range 1130 MHz to 1730 MHz. PSR J0453+1559 was observed for approximately 1 hour a month over a span of 12 months. The data was taken using the Puerto Rico Ultimate Pulsar Processing Instrument (PUPPI), a clone similar to GUPPI at GreenBank Observatory ³ as a back-end, which allows simultaneous processing of the whole band provided by the receiver.

2.4 SOLVING DOUBLE NEUTRON STAR SYSTEM ORBIT

The first sets of data taken on PSR J0453+1559 were from observations that were conducted in a relatively small time frame so it would be possible to get an initial phase connection, which can be used to determine the pulsar’s orbital parameters. In order to build up timing solutions for pulsars, the observations must be spaced closely together so that you can unambiguously account for every rotation of the pulsar. After the initial observations, the observation are then conducted on a monthly basis for a full year. For pulsars in binary systems, the apparent pulse period changes due to time-variable Doppler shifts. These shifts occur as the pulsar moves about the center of mass of the binary system. In order to account for this variation, we must have several observations to determine the pulsars period at each epoch using the period optimisation procedure as described in section 2.3, since it is not possible to use a constant folding period. The orbital parameters need to be taken into account when creating an accurate ephemeris file that can then be used to fold the data. Since the pulsar’s period that these parameters

³<http://safe.nrao.edu/wiki/bin/view/CICADA/GUPPISupportGuide>

are based off is changing drastically over a short time period, it is necessary to attempt to fit the data multiple times to achieve the best fit possible. For a binary orbit, the plot of the observed periods, P_{obs} , versus time can be fitted to the Keplerian model:

$$P_{obs} = P_{int} \left(1 + \frac{V(t)}{c} \right).$$

P_{int} is the intrinsic period of the pulsar and $V(t)$ is its projected velocity along the line of sight as a function of time t .

Using a tool found in PRESTO called `fitorb.py`, it is possible to fit a curve to a set of observed periods of a pulsar ⁴. It is necessary to create a text file that includes the sets of Modified Julian Date (MJD) with the corresponding observed period with its uncertainties. The MJDs that are included in this text file must be relatively consecutive and there must be at least five observing dates. To get a true fit you will most likely have to run `fitorb.py` on this text file multiple times. The initial orbital period calculated using this tool has a large uncertainty due to the fact that if the initial data span is only a week long and the actual orbital period is months long, the run will only be able to fit for week long orbits. As more data is taken on the pulsar and this tool is run additional times throughout the year of observations, the better the fit becomes as longer orbital periods are able to be taken into account.

If the binary system is not a bright one, scientists must use other methods to determine its parameters. Examples of weak pulsars are the ones in globular clusters, which are surrounded by many other stars and gasses causing the scintillation of the

⁴<http://www.cv.nrao.edu/~sransom/presto/>

pulsar's signal and these pulsars are located farther away than the ones within the galaxy. Due to the weaker signal, these pulsars often do not have sufficient data to solve for its orbital parameters. In a paper by Paulo Freire and collaborators, [14], it is demonstrated that for every single observation, it is possible to detect a significant period derivative due to the orbital motion of the system by plotting the recorded periods in \dot{P} - P space. Then you fit an ellipse model to these points to determine the orbital period and projected semi-major axis. Without this technique, it could not be possible to solve for the orbital parameters of weak pulsars.

If the pulsar in a binary system is a strong one, it is possible to use Kepler's laws to derive the five timing model parameters: the orbital period P_b , projected semi-major orbital axis x , orbital eccentricity e , longitude of periastron w and the epoch of periastron passage T_0 . The same procedure is used to solve for these parameters using spectroscopy, the star's radial velocity curve is used rather than the period of the pulsar in binary systems.

After fitting the data points in the from your series of observations, you are now able to decipher the five timing orbital parameters. According to the fit of the PSR J0453+1559, and it has a orbital period of 4.07 days, an eccentricity of 0.1125, and the projected semi-major axis is 14.4668 light-seconds. Now having the orbital parameters you can now get some constraints on the masses of the pulsar and its companion.

2.5 MASS FUNCTION

It is possible to determine the mass of the pulsar and its companion star when they exists in a binary system together. By using classical Keplerian parameters, it is

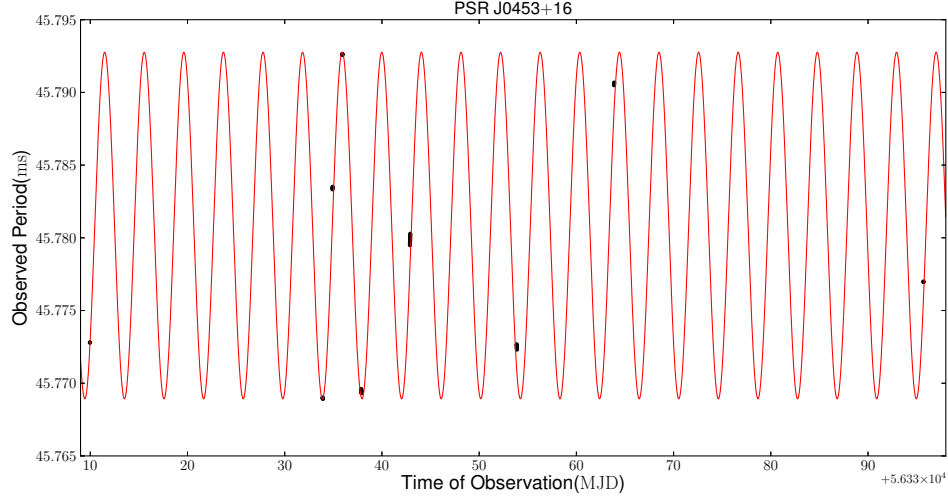


Figure 10: Barycentric period measurements of PSR J0453+1559 vs time. The black dots denote observations and the red curve shows the expected change in observed period due to eccentric orbital motion for the best fit orbit.

possible to incorporate constraints on the mass of the companion. Using the projected semi-major axis and the orbital period, we can work to obtain the mass function of both stars (the derivation of this is below):

$$f(m_p, m_c) = \frac{(m_c \sin i)^3}{(m_p + m_c)^2} = \frac{4\pi^2 x^3}{T_\odot P_b^2}.$$

where $T_\odot = (GM_\odot c^{-3}) = 4.925490947 \mu s$ is a constant, i , is the inclination between the plane of the orbit and the line of sight (which is perpendicular the the observer), x is the projected semi-major axis, P_b is the orbital period and m_p and m_c are the pulsar and comapanion masses respectively. From knowledge of other binary systems, we assume that $m_p = 1.4 M_\odot$, and from this we calculate the constraints on m_c using the mass function and assuming the inclination angle. When i is 90 degrees, the companion mass will be at its minimum.

To derive the mass function, we start with Kepler's third law of planetary motion: the square of the orbital period of a planet is proportional to the cube of the semi-major axis of its orbit:

$$GM = \left(\frac{2\pi}{P_{orb}} \right)^2 a^3. \quad (4)$$

If we algebraically change the total mass, M ,

$$M = m_1 + m_2 = m_1 \left(1 + \frac{m_2}{m_1} \right) = m_1(1 + q), \quad (5)$$

where $q = m_2 / m_1$ and knowing the fact that $m_1 a_1 = m_2 a_2$, the semi-major axis a is re-arranged:

$$a^3 = (a_1 + a_2)^3 = a_2^3 \left(1 + \frac{a_1}{a_2} \right)^3 = a_2^3 \left(1 + \frac{m_2}{m_1} \right)^3 = a_2^3(1 + q)^3. \quad (6)$$

Using these new definitions, we plug them back into Kepler's third law, equation (4).

$$Gm_1(1 + q) = \left(\frac{2\pi}{P_{orb}} \right)^2 a_2^3(1 + q)^3. \quad (7)$$

Now we want to rewrite a_2 as something we can measure. We can use the maximum radial velocity of m_2 : $V_2 = v_2 \sin i$, where v_2 is the orbital velocity of m_2 , to rewrite a_2 . Noting that:

$$P_{orb} = \frac{2\pi}{\omega} = \frac{2\pi a_2}{v_2} = \frac{2\pi a_2 \sin i}{V_2} \quad (8)$$

and rearranging the equation above to get the quantity we desire, we get:

$$a_2 = \frac{P_{orb} V_2}{2\pi \sin i} \quad (9)$$

Substituting this equation back into Kepler's law, we get:

$$Gm_1 = \left(\frac{2\pi}{P_{orb}} \right)^2 \left(\frac{P_{orb} V_2}{2\pi \sin i} \right)^3 (1+q)^2. \quad (10)$$

And, by once again rearranging once again, we get the mass function:

$$\frac{m_1 \sin^3 i}{(1+q)^2} = \frac{P_{orb} V_2^2}{2\pi G}. \quad (11)$$

We were able to successfully determine the five orbital timing model parameters of PSR J0453+1559. The orbital period was determined to be 4.07 days. This means that this system is not a very tight system where it would be possible to measure the Einstein delay and the orbital decay due to the emission of gravitational waves. The eccentricity is 0.11 and the projected semi-major axis of the orbit is 14.5 light seconds.

Using these parameters and the Keplerian mass function, we get the constraint of the masses of the system:

$$f(m_p, m_c) = \frac{(m_c \sin i)^3}{(m_p + m_c)^2} = \frac{4\pi^2 x^3}{T_\odot P_b^2} = 0.1959679(2) M_\odot, \quad (12)$$

Given the orbital eccentricity and this constraint, we are able to make the conclusion that both of the objects in this system are neutron stars. If the companion had instead evolved into a massive white dwarf star, the system would have retained a circu-

lar orbit, which is characteristic of compact accreting systems. This is consistent with the non-detection of an optical counterpart of the system, see Figure 11.

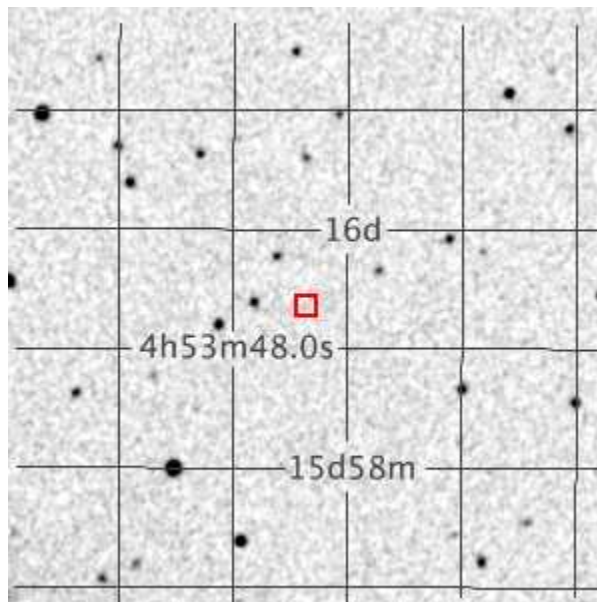


Figure 11: This plot was created by the online Digital Sky Survey, NASA Infrared Science Archive which shows no optical companion near pulsar J0453+1559 within 5 arcminutes.

2.6 SHAPIRO DELAY

For a binary system, in this case a double neutron star system, it is possible to determine the general relativistic Shapiro Delay of the system. The Shapiro delay is an increase in light travel time as it travels past a massive body that is causing space-time to be warped. From binary pulsar systems that have greatly inclined orbits, it is possible to detect a delay in the pulse arrival times when the pulsar is at the superior conjunction with its companion star. Superior conjunction is the time when two astronomical objects appear close to eclipse with each other. By measuring the Shapiro delay it is possible to determine an estimate of the mass of the companion and the inclination angle. You then plug these parameters into the mass function and directly solve for the mass of the pulsar and its companion.

The Shapiro delay was discovered by Irwin Shapiro in 1966 by bouncing radar beams off to the surface of Venus and Mercury. Shapiro was measuring the round trip journey time for light beams when the Earth, Sun, and Venus were aligned. The experiment showed that the expected time delay, due to the presence of heavy objects, of the radar signal as it traveled from Earth to Venus was about 200 microseconds [30]. The experiment was done using the MIT Haystack radar antenna. This experiment has been repeated many times, each time with more precise measurements.

To determine the Shapiro delay of PSR J0453+1559, a special observation session proposal was submitted to the Arecibo Observatory, due to the fact the Shapiro delay can only be observed in certain times. It is possible to see the Shapiro delay as a peak in a TOA residuals versus orbital phase plot. This is due to the fact that the Shapiro

delay is an increase in light travel time through the curved space-time near a massive body, see Figure 12. Calculation of the Shapiro delay experienced by PSR J0453+1559 were done during an observation conducted between Aug 23 through Aug 27, 2014. This experiment lasted for five consecutive days, starting and ending with a day where superior conjunction occurs. Each observation lasted about two hours. A well detected Shapiro delay allows for a precise measurement of the total mass of the system and also helps constrain the individual masses of the pulsar and the companion neutron star. In Figure 13 you can see the observed Shapiro delay of this binary system.

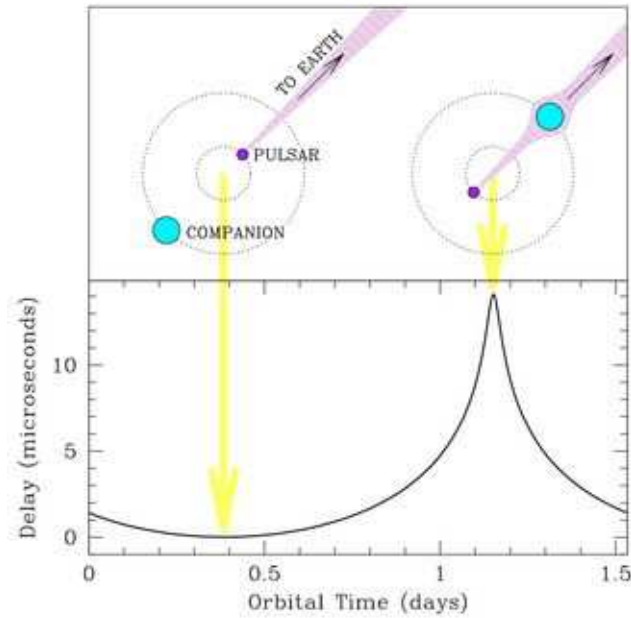


Figure 12: Example of a Shapiro Delay for a pulsar orbiting a massive companion, as the pulses of the pulsar are in line of sight of the companion the TOAs arrive earlier creating a spike in the plot.⁵

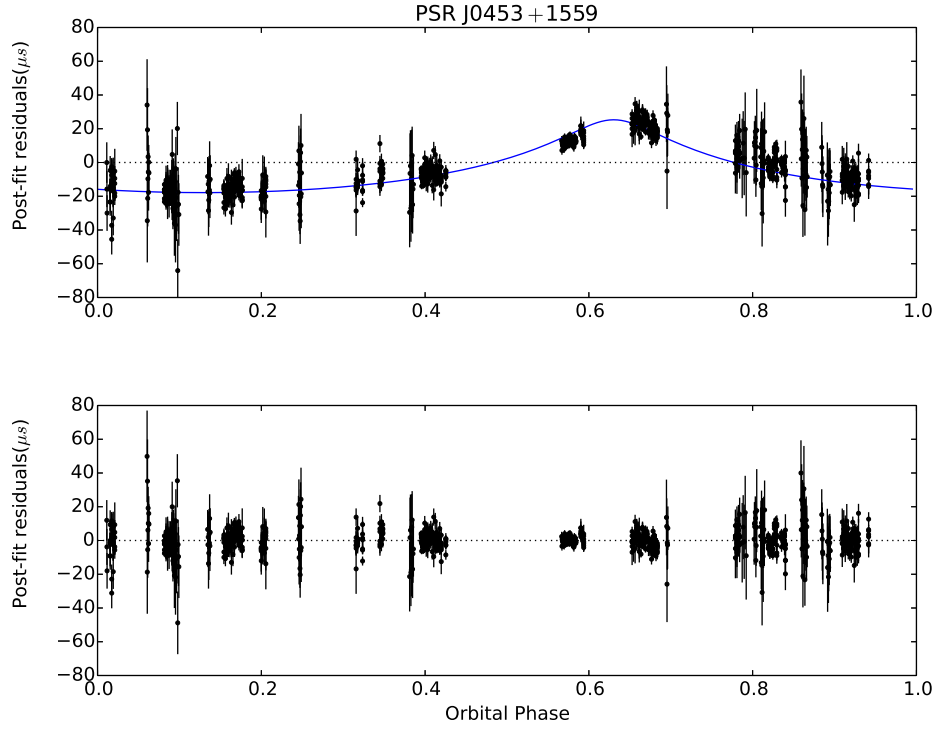


Figure 13: This plot shows the timing residuals versus its orbital phase of the binary system in which pulsar J0453+1559 is in. The top graph shows the detection of the Shapiro Delay which enables to constrain and measure precise mass measurements of the total mass and companion mass of the system.

2.7 POST-KEPLERIAN PARAMETERS AND RELATIVISTIC PARAMETERS

Assuming general relativity is correct, you can derive the five “Post-Keplerian” parameters [5]. The five parameters are: the rate of change of periastron in degree per year, $\dot{\omega}$, the orbital decay of the system due to the outpouring of gravitational radiation, \dot{P}_b , the gravitational redshift of the system coming from general relativity, γ , and two additional parameters measured from the Shapiro delay, r and s . γ gives information about the time in which the object’s electromagnetic radiation is in a strong gravitational field, causing a change in the recorded frequency in a weaker gravitational field. These parameters were first succesfully measured using the first double neutron star system, PSR B1913+16 [21] [35].

$$\dot{\omega} = 3T_{\odot}^{\frac{2}{3}} \left(\frac{P_b}{2\pi} \right)^{-\frac{5}{3}} (m_p + m_c)^{\frac{2}{3}} \frac{1}{(1 - e^2)} \quad (13)$$

$$\gamma = T_{\odot}^{\frac{2}{3}} \left(\frac{P_b}{2\pi} \right)^{\frac{1}{3}} e \frac{m_c(m_p + 2m_c)}{(m_p + m_c)^{\frac{4}{3}}} \quad (14)$$

$$\dot{P}_b = -\frac{192\pi}{5} T_{\odot}^{\frac{5}{3}} \left(\frac{P_b}{2\pi} \right)^{-\frac{5}{3}} \frac{(1 + \frac{73}{24}e^2 + \frac{37}{96}e^4)}{(1 - e^2)^{\frac{7}{2}}} \frac{m_p m_c}{(m_p + m_c)^{\frac{-1}{3}}} \quad (15)$$

$$r = T_{\odot} m_c \quad (16)$$

$$s = T_{\odot}^{\frac{-1}{3}} \left(\frac{P_b}{2\pi} \right)^{\frac{-2}{3}} x \frac{(m_p + m_c)^{\frac{2}{3}}}{m_c} \quad (17)$$

For PSR J0453+1559, it was possible to determine three Post-Keplerian parameters.

They were $\dot{\omega}$, r , and s .

CHAPTER 3

RESULTS OF J0453+1559

This paper will be submitted to the Astrophysical Journal.

Pulsar J0453+1559, An Asymmetric Double Neutron Star System

J.G. Martinez¹, K. Stovall^{1,2}, P.C.C. Freire³, J.S. Deneva⁴, F.A. Jenet¹,

M.A. McLaughlin⁵, S.D. Bates⁵, M. Bagchi⁵

¹Center for Advanced Radio Astronomy, University of Texas at Brownsville, One West University Boulevard, Brownsville, TX 78520

²Department of Physics and Astronomy, University of New Mexico, Albuquerque, New Mexico 87131

³Max-Planck-Institut für Radioastronomie, Auf dem Hügel 69, D-53121 Bonn, Germany

⁴Arecibo Observatory, HC3 Box 53995, Arecibo, PR 00612

⁵Department of Physics, West Virginia University, 111 White Hall, Morgantown, WV 26506

3.1 ABSTRACT

We report the results of a study of PSR J0453+1559, a new binary pulsar discovered in the Arecibo All-Sky 327 MHz Drift Pulsar Survey. Our timing observations of the radio pulsar in the system, PSR J0453+1559, span a period of about 300 days, which allowed precise measurement of its spin period (45.7 ms) and its derivative $(1.85 \pm 0.13) \times 10^{-19} \text{ ss}^{-1}$; from these we derive a characteristic age of $\sim 3.9 \times 10^6$ years and a magnetic field of $\sim 2.9 \times 10^9$ G. These numbers indicate that this pulsar was mildly recycled by accretion of matter from the progenitor of the companion star. The system has an eccentric ($e = 0.11$) 4.07-day orbit. This eccentricity allows a highly significant measurement of the rate of advance of periastron, $\dot{\omega} = 0.0379 \pm 0.0005^\circ \text{yr}^{-1}$, which implies a total system mass $M = 2.73 \pm 0.006 M_\odot$. We also detect a faint trace of the Shapiro delay, which allows an estimate of the individual masses: $m_p = 1.54 \pm 0.006 M_\odot$ and $m_c = 1.19 \pm 0.011 M_\odot$, respectively. These masses, along with the orbital eccentricity, suggest that PSR J0453+1559 is a double neutron star system with a large mass asymmetry. The expected coalescence time due to emission of gravitational waves is $\sim 1.4 \text{ Tyr}$, $\sim 10^2$ times larger than the age of the universe.

3.2 INTRODUCTION

Double neutron star (DNS) systems are rare and valuable physical laboratories that can be used to precisely test gravity theories. The first such system, PSR B1913+16, provided evidence for orbital decay due to the emission of gravitational waves as predicted by General Relativity GR, [21] & [35]. Since the discovery of PSR B1913+16, eight additional DNS systems have been discovered Table 2, including one such system in

which both neutron stars are detectable as radio pulsars, PSRs J0737-3039A and J0737-3039B [6]. This system provides one of the best available tests of GR and alternative theories of gravity in the strong-field regime.

DNS systems begin as two high-mass stars. The higher-mass star will undergo a supernova explosion resulting in a neutron star and a high-mass companion. Prior to the supernova of the companion, there is typically a period of mass transfer from the companion onto the neutron star and the system can be detected as a high-mass X-ray binary. Eventually, the companion will undergo a supernova explosion, leaving behind two neutron stars: the older might be detected as a mildly recycled pulsar which was spun up by accretion from the progenitor of the younger star, the younger might be detected as a normal pulsar. In the rare case that the system survives both supernovae, the result is a DNS.

In this letter, we report the initial timing solution for the newly discovered PSR J0453+1559, which appears to be a new DNS system. PSR J0453+1559 has a spin period of 45.8 ms and a DM of $30.3 \text{ cm}^{-3}\text{pc}$ and was discovered in the Arecibo 327 MHz Drift Pulsar Survey [12], which began in 2010. The survey targets the declination range accessible to the Arecibo telescope, $-1^\circ - 38^\circ$, and has an effective integration time of 1 minute. The survey is sensitive to very tight relativistic binaries even with only moderate acceleration searches. To date, 44 new radio pulsars have been discovered. In section 2, we describe the timing procedure and in section 3, we present the timing parameters of this new system.

Table 2: Double Neutron Star Systems known in the Universe

Pulsar	Period (ms)	P_b (days)	x (lt-sec)	e	M_T (M_\odot)	M_p (M_\odot)	M_c (M_\odot)	Reference
J0737-3039A	22.699	0.1022	1.415	0.0877	2.587	1.338		[6]
J0737-3039B	2773.461		1.516				1.249	
B1534+12	37.904	0.420	3.729	0.2736	2.678	1.333	1.345	[36]
J1756-2251	28.461	0.3196	2.756	0.1805	2.57	1.312	1.258	[13]
J1906+0746	144.071	0.1659	1.419	0.0853	2.6133	1.323	1.290	[24]
B1913+16	59.031	0.3229	2.341	0.617	2.828	1.439	1.388	[21]
B2127+11C	30.529	0.3353	2.518	0.6814	2.712	1.358	1.354	[2]
J1829+2456	41.009	1.76	7.236	0.1391	2.5	1.38	1.22	[7]
J1518+4904	40.935	8.634	0.2495	2.7183	2.62			[29]
J1811-1736	104.1	18.779	34.782	0.828	2.57			[26]
J0453+1559	45.782	4.072	14.467	0.1125	2.73	1.54	1.19	

3.3 OBSERVATIONS AND DATA REDUCTION

PSR J0453+1559 was observed with the L-band receiver of the 305-m Arecibo radio telescope for ~ 1 hour once a month in a span of 10 months, using the Puerto Rico Ultimate Pulsar Processing Instrument (PUPPI), a clone similar to GUPPI at GreenBank Observatory ¹ as a back-end, which allows simultaneous processing of the whole band provided by the receiver, from 1130 to 1730 MHz.

The first six months' observations were taken in search mode, this continued until we derived an ephemeris that was capable of predicting the pulsar spin phase. Subsequent observations were taken in coherent dedispersion mode, which coherently dedisperses and folds the data online, effectively removing the dispersive effects of the interstellar medium.

In figure 14, we can see clearly the benefits of using this technique: the main pulse has a sharp feature, which would be undetectable without coherent dedispersion. This feature contributes to the good precision timing of this pulsar discussed in later in the

¹<http://safe.nrao.edu/wiki/bin/view/CICADA/GUPPISupportGuide>

text.

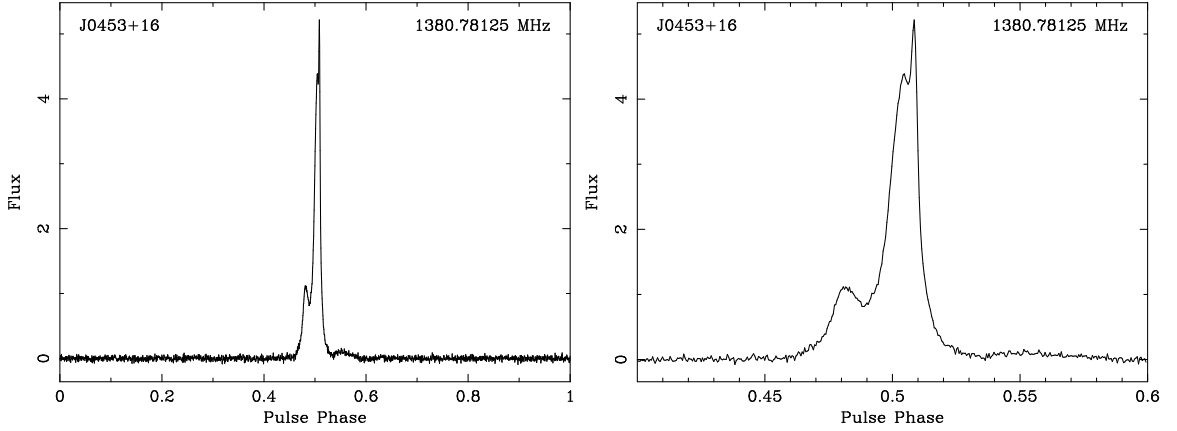


Figure 14: *Left*: Pulse profile of PSR J0453+1559 at 1380 MHz, obtained in a 20 min observation with the L-wide receiver of Arecibo Observatory. *Right*: Zooming in on the pulse profile, we can see more clearly a very sharp feature in the main pulse. This is one of the reasons for the excellent timing precision of this pulsar.

The dedispersed pulse profiles obtained with 5 minutes of data are then cross-correlated with a low-noise template to derive 494 topocentric pulse times of arrival (TOAs), as described in [32] and implemented in the `PSRCHIVE` software [20] & [34].

We then used `tempo` to correct the TOAs using the Arecibo Observatory’s clock corrections and to convert them to the solar system barycentre. To do this, the motion of the radio telescope relative to the Earth was calculated using the data from the International Earth Rotation Service, and to the barycentre using the DE421 solar system ephemeris ².

Finally, the difference between the measured TOAs and those predicted by a model of the spin and the orbit of the pulsar is minimized by `tempo`, by varying the parameters in the model. The parameters that best fit the data are presented in Table 3. To model the orbit, we used the DDGR model described by [9] & [10], which assumes the

²<ftp://ssd.jpl.nasa.gov/pub/eph/planets/ioms/de421.iom.v1.pdf>

validity of GR to derive the masses of the components and the system, and the DDH model described by [16], which like the DD model allows a fit for the post-Keplerian parameters, but includes an optimized description of the Shapiro delay.

The residuals (TOA - model prediction) associated with this model are displayed in figure 15. There are no unmodeled trends in the residuals, either as a function of time or of orbital phase, which implies that the model in Table 3 described the data well. The residual root mean square is $2.8 \mu\text{s}$, which represents a fraction of 6×10^{-5} of the spin period.

Table 3: Timing solutions for PSR J0453+1559.

Timing Parameters	
Right Ascension, α (J2000)	04:53:45.4138(10)
Declination, δ (J2000)	+15:59:21.286(57)
Pulsar Period, P (s)	0.04578181616(43)
Period Derivative, \dot{P} (s s^{-1})	1.85(6)E-19
Dispersion Measure, DM (pc cm^{-3})	30.305(4)
Span of Timing Data (MJD)	56339-56896
Number of TOAs	953
RMS Residual (μs)	2.83
Binary Parameters	
Orbital Period, P_b (days)	4.07246858(73)
Projected Semi-major Axis of the pulsar orbit, x (lt-s)	14.46682(16)
Epoch of Periastron, T_0 (MJD)	56425.703353911
Orbital Eccentricity, e	0.11251847(80)
Longitude of Periastron, ω ($^\circ$)	223.06940(86)
Total Mass, M (M_\odot)	2.732(6)
Companion Mass, m_c (M_\odot)	1.19(1)
Derived Parameters	
Galactic Longitude, l	184.1246
Galactic Latitude, b	-17.1368
DM Derived Distance, d (kpc)	1.0
Surface Magnetic Field Strength, B_0 (10^9 Gauss)	2.91
Characteristic Age, τ_c (Myr)	3.9
Pulsar mass, m_p (M_\odot)	1.54(5)
Orbital inclination, i ($^\circ$)	~ 73

The parameters in Table 3 (the pulsar's ephemeris) include a precise position in the sky, which allows for optical follow-up. No optical counterpart to the system is

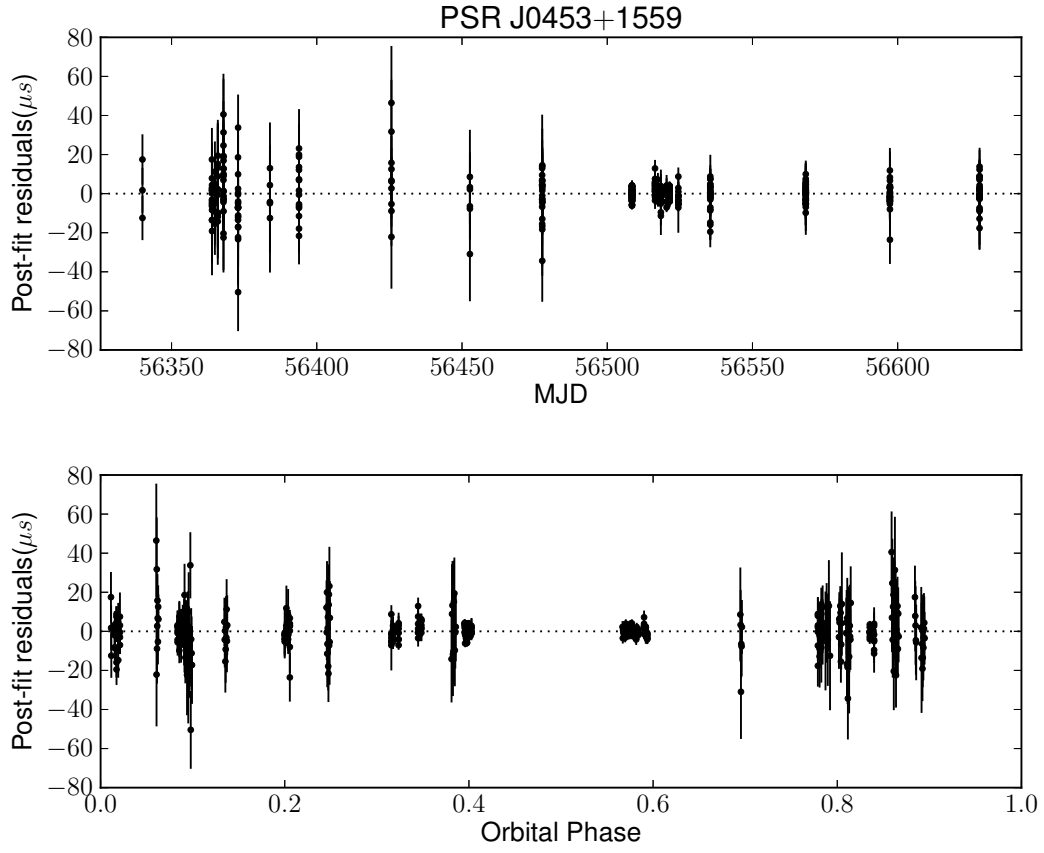


Figure 15: The top plot is Residuals vs. MJD and the lower plot is the Residuals vs. Orbital Phase.

detectable in the online Digital Sky Survey.

The ephemeris also includes the pulsar’s spin period and its derivative $(1.87 \pm 0.13) \times 10^{-19} \text{ ss}^{-1}$; from these we derive a characteristic age of $\sim 3.9 \times 10^6$ years and a magnetic field of $\sim 2.9 \times 10^9$ G. These numbers are similar to what we observe for other pulsars with massive companions, and they indicate that this pulsar was mildly recycled by accretion of matter from the progenitor of the current companion star.

The ephemeris also includes very precise orbital parameters. The orbital period of 4.07 days, i.e., this is not a tight system where we might be able to measure the Einstein

delay and the orbital decay due to the emission of gravitational waves. The eccentricity is 0.11 and the projected semi-major axis of the orbit is 14.5 light seconds. From this we can derive the Keplerian mass function:

$$f(m_p, m_c) = \frac{(m_c \sin i)^3}{(m_p + m_c)^2} = \frac{4\pi^2 x^3}{T_\odot P_b^2} = 0.1959679(2) M_\odot, \quad (1)$$

where $T_\odot = (GM_\odot c^{-3}) = 4.925490947 \mu\text{s}$ is a solar mass in time units, i is the inclination between the plane of the orbit and the line of sight, x is in light seconds, P_b is in seconds and the pulsar and companion masses m_p and m_c , are in solar masses. If we assume for the pulsar a mass of $1.4 M_\odot$ and maximum and median orbital inclinations ($i = 90^\circ, 60^\circ$) we obtain minimum and median companion masses of 1.05 and 1.30 M_\odot , i.e., the companion is relatively massive. Given the orbital eccentricity, this is likely to be a neutron star – if the companion had evolved into a massive white dwarf star, there would be at no instance the sudden mass loss associated with a supernova explosion, and the system would thus have retained the circular orbit that is characteristic of compact accreting systems. This is consistent with the non-detection of an optical counterpart of the system.

We have searched for radio pulsations from this companion in the early observations, which were taken in search mode. These were dedispersed at the same DM as PSR J0453+1559 and then searched with the PRESTO pulsar search code³. The companion was not detected as a radio pulsar.

This orbital eccentricity allows a detection of the the advance of periastron, $\dot{\omega}$. If

³<http://www.cv.nrao.edu/~sransom/presto/>

we assume this to be purely relativistic, then it depends only on the total mass of the system M and Keplerian orbital parameters, which are already known precisely [?]:

$$\dot{\omega} = 3T_{\odot}^{\frac{2}{3}} \left(\frac{P_b}{2\pi} \right)^{-\frac{5}{3}} \frac{1}{1-e^2} M^{\frac{2}{3}}. \quad (2)$$

This yields $M = 2.732 \pm 0.006 \text{ M}_{\odot}$, within the mass range of currently known DNS systems.

PSR J0453+1559

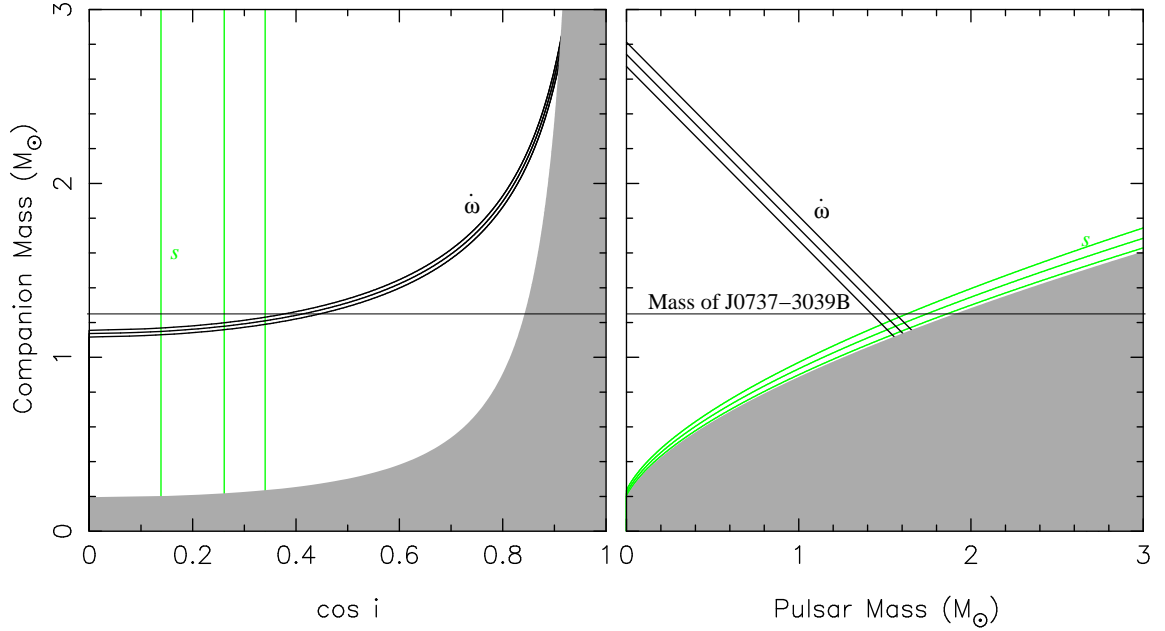


Figure 16: Current constraints from timing of PSR J0453+1559. Each triplet of lines corresponds to the nominal and $\pm 1\sigma$ uncertainties of the post-Keplerian parameters, which are: the rate of advance of periastron $\dot{\omega}$ and the “Shape” parameter for the Shapiro delay, s , which in general relativity is $\sin i$, where i is the orbital inclination. *Left:* $M_c - \cos i$ plane. The gray region is excluded by the physical constraint $M_p > 0$. *Right:* $M_c - M_p$ plane. The gray region is excluded by the mathematical constraint $\sin i \leq 0$.

We also detect a trace of the Shapiro delay. In the DDH solution, the orthometric amplitude h_3 is detected to about $3\text{-}\sigma$ significance, which implies that the orbital incli-

nation must be relatively high. The individual masses cannot be determined with any certainty using the Shapiro delay alone. However, in combination with the total mass constraint, it allows a determination of the component masses, as shown in figure ??.

Using the DDGR model, which uses all these effects in a self-consistent way, we obtain $m_p = 1.54 \pm 0.05 \text{ M}_\odot$, $m_c = 1.19 \pm 0.01 \text{ M}_\odot$ and $i \sim 73^\circ$ respectively. This suggests that there is a large mass asymmetry in the system.

The mass asymmetry observed in this DNS is the second case known if the low mass for PSR J1518+4904 is confirmed [23], and the first case where we have a precise mass measurement for the components of such a system, or also for any wide DNS. Unlike PSR J1518+4904, here it is the mildly recycled pulsar that is most massive and the second formed NS that is less massive. The accretion episode in these systems is very short lived and therefore the NS masses are similar to their masses at the instant of formation.

Until now, most well measured NS masses in DNS systems fell on a narrow range between 1.23 and 1.44 M_\odot [35] & [13]. This had lead to speculation that all NSs might be born within this narrow band, and that the large masses observed in some MSPs like PSR J1903+0327 [15], PSR J1614–2230 [11] and PSR J0348+0432 [3] are due to accrtion. However, from an analysis of the evolution of PSR J1614–2230, [31] had already suggested that at least some NSs must be born more massive than 1.44 M_\odot . The result presented here indicates that, as suggested by the latter analysis, the range of NS birth masses is indeed substantially wider than the 1.23 and 1.44 M_\odot .

The mass asymmetry is very important in itself, particularly if the lighter NS has

a mass smaller than 0.8 of that of the most massive component, as is the case in the J0453+1559 system. When such a system merges, the lighter (and larger) NS is tidally disrupted by the smaller, more massive NS. According to recent simulations (references later), such mergers result in a much larger release of heavy elements to space, possibly explaining the heavy element abundances in our galaxy. This would also have an impact for searches of gravitational waves in ground-based GW detectors, since we can no longer assume that the NSs in NS-NS have similar masses. In such systems dipolar gravitational wave emission could theoretically become important at the later stages of the merger; however this possibility is already significantly constrained by the measurement of the orbital decay of PSR J0348+0432 [3].

However, asymmetric DNSs can only be an explanation for heavy element abundances if they form with an orbital period that is small enough for them to merge well within a Hubble time. The existence of systems like PSR J1518+4904 and J0453+1559 have very large merger times - in the case of J0453+1559, this is more 1430 Gyr (1.43 Tyr), which is almost exactly 100 times the current age of the universe (and even much longer for PSR J1518+4904). This implies that similar systems cannot explain the heavy element abundances in the universe. But given the wide range of NS masses observed in the wider system, it is possible that similarly asymmetric compact systems might be found in the future.

REFERENCES

- [1] Book Review: Unsolved problems in astrophysics / Princeton U Press, 1997. , 388:37, July 1997.
- [2] S. Anderson, P. Gorham, S. Kulkarni, T. Prince, and A. Wolszczan. PSR 2127+11C. , 4772:1, April 1989.
- [3] J. Antoniadis, P. C. C. Freire, N. Wex, T. M. Tauris, R. S. Lynch, M. H. van Kerkwijk, M. Kramer, C. Bassa, V. S. Dhillon, T. Driebe, J. W. T. Hessels, V. M. Kaspi, V. I. Kondratiev, N. Langer, T. R. Marsh, M. A. McLaughlin, T. T. Pennucci, S. M. Ransom, I. H. Stairs, J. van Leeuwen, J. P. W. Verbiest, and D. G. Whelan. A Massive Pulsar in a Compact Relativistic Binary. *Science*, 340:448, April 2013.
- [4] D. C. Backer, S. R. Kulkarni, C. Heiles, M. M. Davis, and W. M. Goss. A millisecond pulsar. , 300:615–618, December 1982.
- [5] R. Blandford and S. A. Teukolsky. Arrival-time analysis for a pulsar in a binary system. , 205:580–591, April 1976.
- [6] M. Burgay, N. D’Amico, A. Possenti, R. N. Manchester, A. G. Lyne, B. C. Joshi, M. A. McLaughlin, M. Kramer, J. M. Sarkissian, F. Camilo, V. Kalogera, C. Kim, and D. R. Lorimer. An increased estimate of the merger rate of double neutron stars from observations of a highly relativistic system. , 426:531–533, December 2003.
- [7] D. J. Champion, D. R. Lorimer, M. A. McLaughlin, J. M. Cordes, Z. Arzoumanian, J. M. Weisberg, and J. H. Taylor. PSR J1829+2456: a relativistic binary pulsar. , 350:L61–L65, June 2004.

- [8] F. Crawford, V. M. Kaspi, R. N. Manchester, A. G. Lyne, F. Camilo, and N. D’Amico. Radio Pulsars in the Magellanic Clouds. , 553:367–374, May 2001.
- [9] T. Damour and N. Deruelle. General relativistic celestial mechanics of binary systems. I. The post-Newtonian motion. *Ann. Inst. Henri Poincaré Phys. Théor.*, Vol. 43, No. 1, p. 107 - 132, 43:107–132, 1985.
- [10] T. Damour and N. Deruelle. General relativistic celestial mechanics of binary systems. II. The post-Newtonian timing formula. *Ann. Inst. Henri Poincaré Phys. Théor.*, Vol. 44, No. 3, p. 263 - 292, 44:263–292, 1986.
- [11] P. B. Demorest, T. Pennucci, S. M. Ransom, M. S. E. Roberts, and J. W. T. Hessels. A two-solar-mass neutron star measured using Shapiro delay. , 467:1081–1083, October 2010.
- [12] J. S. Deneva, K. Stovall, M. A. McLaughlin, S. D. Bates, P. C. C. Freire, J. G. Martinez, F. Jenet, and M. Bagchi. Goals, Strategies and First Discoveries of AO327, the Arecibo All-sky 327 MHz Drift Pulsar Survey. , 775:51, September 2013.
- [13] A. J. Faulkner, M. Kramer, A. G. Lyne, R. N. Manchester, M. A. McLaughlin, I. H. Stairs, G. Hobbs, A. Possenti, D. R. Lorimer, N. D’Amico, F. Camilo, and M. Burgay. PSR J1756-2251: A New Relativistic Double Neutron Star System. , 618:L119–L122, January 2005.
- [14] P. C. Freire, M. Kramer, A. G. Lyne, F. Camilo, R. N. Manchester, and N. D’Amico. Detection of Ionized Gas in the Globular Cluster 47 Tucanae. , 557:L105–L108, August 2001.

- [15] P. C. C. Freire, C. G. Bassa, N. Wex, I. H. Stairs, D. J. Champion, S. M. Ransom, P. Lazarus, V. M. Kaspi, J. W. T. Hessels, M. Kramer, J. M. Cordes, J. P. W. Verbiest, P. Podsiadlowski, D. J. Nice, J. S. Deneva, D. R. Lorimer, B. W. Stappers, M. A. McLaughlin, and F. Camilo. On the nature and evolution of the unique binary pulsar J1903+0327. , 412:2763–2780, April 2011.
- [16] P. C. C. Freire and N. Wex. The orthometric parametrization of the Shapiro delay and an improved test of general relativity with binary pulsars. , 409:199–212, November 2010.
- [17] T. Gold. Rotating Neutron Stars and the Nature of Pulsars. , 221:25–27, January 1969.
- [18] J. W. T. Hessels, S. M. Ransom, I. H. Stairs, P. C. C. Freire, V. M. Kaspi, and F. Camilo. A Radio Pulsar Spinning at 716 Hz. *Science*, 311:1901–1904, March 2006.
- [19] A. Hewish, S. J. Bell, J. D. H. Pilkington, P. F. Scott, and R. A. Collins. Observation of a Rapidly Pulsating Radio Source. , 217:709–713, February 1968.
- [20] A. W. Hotan, W. van Straten, and R. N. Manchester. PSRCHIVE and PSRFITS: An Open Approach to Radio Pulsar Data Storage and Analysis. , 21:302–309, 2004.
- [21] R. A. Hulse and J. H. Taylor. Discovery of a pulsar in a binary system. , 195:L51–L53, January 1975.
- [22] John David Jackson.
- [23] G. H. Janssen, B. W. Stappers, M. Kramer, D. J. Nice, A. Jessner, I. Cognard, and M. B. Purver. Multi-telescope timing of PSR J1518+4904. , 490:753–761, November

2008.

- [24] D. R. Lorimer, I. H. Stairs, P. C. Freire, J. M. Cordes, F. Camilo, A. J. Faulkner, A. G. Lyne, D. J. Nice, S. M. Ransom, Z. Arzoumanian, R. N. Manchester, D. J. Champion, J. van Leeuwen, M. A. McLaughlin, R. Ramachandran, J. W. Hessels, W. Vlemmings, A. A. Deshpande, N. D. Bhat, S. Chatterjee, J. L. Han, B. M. Gaensler, L. Kasian, J. S. Deneva, B. Reid, T. J. Lazio, V. M. Kaspi, F. Crawford, A. N. Lommen, D. C. Backer, M. Kramer, B. W. Stappers, G. B. Hobbs, A. Possenti, N. D’Amico, and M. Burgay. Arecibo Pulsar Survey Using ALFA. II. The Young, Highly Relativistic Binary Pulsar J1906+0746. , 640:428–434, March 2006.
- [25] A. G. Lyne, A. Brinklow, J. Middleditch, S. R. Kulkarni, and D. C. Backer. The discovery of a millisecond pulsar in the globular cluster M28. , 328:399–401, July 1987.
- [26] A. G. Lyne, F. Camilo, R. N. Manchester, J. F. Bell, V. M. Kaspi, N. D’Amico, N. P. F. McKay, F. Crawford, D. J. Morris, D. C. Sheppard, and I. H. Stairs. The Parkes Multibeam Pulsar Survey: PSR J1811-1736, a pulsar in a highly eccentric binary system. , 312:698–702, March 2000.
- [27] A. G. Lyne and F. Graham-Smith. *Pulsar Astronomy*. July 2005.
- [28] F. Pacini. Rotating Neutron Stars, Pulsars and Supernova Remnants. , 219:145–146, July 1968.
- [29] R. W. Sayer, D. J. Nice, and J. H. Taylor. The Green Bank Northern Sky Survey for Fast Pulsars. , 474:426, January 1997.
- [30] I. I. Shapiro. New Method for the Detection of Light Deflection by Solar Gravity.

- Science*, 157:806–808, August 1967.
- [31] T. M. Tauris, N. Langer, and M. Kramer. Formation of millisecond pulsars with CO white dwarf companions - I. PSR J1614-2230: evidence for a neutron star born massive. , 416:2130–2142, September 2011.
 - [32] J. H. Taylor. Pulsar Timing and Relativistic Gravity. *Royal Society of London Philosophical Transactions Series A*, 341:117–134, October 1992.
 - [33] S. E. Thorsett, Z. Arzoumanian, and J. H. Taylor. PSR B1620-26 - A binary radio pulsar with a planetary companion? , 412:L33–L36, July 1993.
 - [34] W. van Straten, P. Demorest, and S. Osłowski. Pulsar Data Analysis with PSRCHIVE. *Astronomical Research and Technology*, 9:237–256, July 2012.
 - [35] J. M. Weisberg, D. J. Nice, and J. H. Taylor. Timing Measurements of the Relativistic Binary Pulsar PSR B1913+16. , 722:1030–1034, October 2010.
 - [36] A. Wolszczan. A nearby 37.9-ms radio pulsar in a relativistic binary system. , 350:688–690, April 1991.
 - [37] A. Wolszczan and D. A. Frail. A planetary system around the millisecond pulsar PSR1257 + 12. , 355:145–147, January 1992.